

Destroy this report when it is no longer needed. Do not return to sender.

PLEASE NOTIFY THE DEFENSE NUCLEAR AGENCY,
ATTN: CSTI, 6801 TELEGRAPH ROAD, ALEXANDRIA, VA
22310-3398, IF YOUR ADDRESS IS INCORRECT, IF YOU
WISH IT DELETED FROM THE DISTRIBUTION LIST, OR
IF THE ADDRESSEE IS NO LONGER EMPLOYED BY YOUR
ORGANIZATION.



DISTRIBUTION LIST UPDATE

This mailer is provided to enable DNA to maintain current distribution lists for reports. (We would appreciate your providing the requested information.)

- Add the individual listed to your distribution list.
- Delete the cited organization/individual.
- Change of address.

NOTE:
Please return the mailing label from the document so that any additions, changes, corrections or deletions can be made easily. For distribution cancellation or more information call DNA/IMAS (703) 325-1036.

NAME: _____

ORGANIZATION: _____

OLD ADDRESS

CURRENT ADDRESS

_____	_____
_____	_____
_____	_____

TELEPHONE NUMBER: () _____

DNA PUBLICATION NUMBER/TITLE

CHANGES/DELETIONS/ADDITIONS, etc.)
(Attach Sheet if more Space is Required)

_____	_____
_____	_____
_____	_____

DNA OR OTHER GOVERNMENT CONTRACT NUMBER: _____

CERTIFICATION OF NEED-TO-KNOW BY GOVERNMENT SPONSOR (if other than DNA): _____

SPONSORING ORGANIZATION: _____

CONTRACTING OFFICER OR REPRESENTATIVE: _____

SIGNATURE: _____

CUT HERE AND RETURN



REPORT DOCUMENTATION PAGE

Form Approved
OMB No. 0704-0188

Public reporting burden for this collection of information is estimated to average 1 hour per response including the time for reviewing instructions, searching existing data sources, gathering and maintaining the data needed, and completing and reviewing the collection of information. Send comments regarding this burden estimate or any other aspect of this collection of information, including suggestions for reducing this burden, to Washington Headquarters Services Directorate for Information Operations and Reports, 1215 Jefferson Davis Highway, Suite 1204, Arlington, VA 22202-4302, and to the Office of Management and Budget, Paperwork Reduction Project (0704-0188), Washington, DC 20503

1. AGENCY USE ONLY (Leave blank)	2. REPORT DATE <p style="text-align: center;">941201</p>	3. REPORT TYPE AND DATES COVERED <p style="text-align: center;">Project Officer's Report 930616 - 931231</p>	
4. TITLE AND SUBTITLE <p style="text-align: center;">Hazard Evaluation on ANFO Charges</p>		5. FUNDING NUMBERS <p style="text-align: center;">C -DNA 001-93-C-0039</p>	
6. AUTHOR(S) <p style="text-align: center;">Doug Olson and Marvin Banks</p>			
7. PERFORMING ORGANIZATION NAME(S) AND ADDRESS(ES) University of New Mexico Engineering Research Institute P.O. Box 25 Albuquerque, NM 87131		8. PERFORMING ORGANIZATION REPORT NUMBER EMRTC Report # FR-93-20	
9. SPONSORING/MONITORING AGENCY NAME(S) AND ADDRESS(ES) Defense Nuclear Agency 6801 Telegraph Road Alexandria, VA 22310-3398 FCTT/Rinehart		10. SPONSORING/MONITORING AGENCY REPORT NUMBER POR 7547	
11. SUPPLEMENTARY NOTES			
12a. DISTRIBUTION/AVAILABILITY STATEMENT Approved for public release; distribution is unlimited.		12b. DISTRIBUTION CODE	
13. ABSTRACT (<i>Maximum 200 words</i>) The purpose of this work was to determine the potential thermal hazards from self-heating of large ANFO charges. To accomplish this objective, the thermal stability of ANFO was determined from measurements of the critical temperature at three sample sizes: 40 mg, 25 g, and 25 kg. The effective thermal conductivity of solid ANFO at density 0.85 g/cm ³ was measured as 0.11 W/(m K) using a specific heat value of 1.5 J/(g K). The cook-off data were used to determine the decomposition rate coefficient from 168 to 297°C—a range covering over five decades in reaction rate. The resulting Arrhenius rate constant expression was determined. These data were compared with previous studies on AN/fuel mixtures. The Experimentally-determined ANFO parameters were incorporated into two models to investigate the potential for thermal runaway of 2,400 and 4,800 ton charges. Overall, the work reported here showed ANFO to be a highly thermally stable energetic material, suitable for use in large conventional explosive charges. The data measured in this work allow predictions of minimum thermal runaway conditions for ANFO charges of various sizes and for various initial conditions. If the initial temperature			
14. SUBJECT TERMS ANFO Large Charge Thermal Hazard Blasting Agent Thermal Stability High Explosive Ammonium Nitrate/Fuel Oil		15. NUMBER OF PAGES <p style="text-align: center;">52</p>	
		16. PRICE CODE	
17. SECURITY CLASSIFICATION OF REPORT <p style="text-align: center;">UNCLASSIFIED</p>	18. SECURITY CLASSIFICATION OF THIS PAGE <p style="text-align: center;">UNCLASSIFIED</p>	19. SECURITY CLASSIFICATION OF ABSTRACT <p style="text-align: center;">UNCLASSIFIED</p>	20. LIMITATION OF ABSTRACT <p style="text-align: center;">SAR</p>

UNCLASSIFIED

SECURITY CLASSIFICATION OF THIS PAGE

CLASSIFIED BY:

N/A since Unclassified.

DECLASSIFY ON:

N/A since Unclassified.

13. ABSTRACT (Continued)

of ANFO loaded into a container [e.g., a hemisphere of 2,400 tons (10 meters radius, 70 feet in diameter)] is near ambient, the models indicate that no credible external heating is likely to bring the material to a runaway condition. The remaining hazards are mainly from a large fire at the surface or inside the ANFO, or nearby in some other fuel, or from accidental detonation of some other explosive (e.g., a high explosive booster charge) near the ANFO.

SUMMARY

The purpose of this work was to determine the potential thermal hazards from self-heating of large ANFO charges.

To accomplish this objective, the thermal stability of ANFO was determined from measurements of the critical temperature (i.e., the minimum temperature at which thermal runaway occurs) at three sample sizes: 40 mg, 25 g, and 25 kg. The effective thermal conductivity of solid ANFO at density 0.85 g/cm^3 was measured as 0.11 W/(m K) using a specific heat value of 1.5 J/(g K) . The cook-off data were used to determine the decomposition rate coefficient from 168 to 297°C —a range covering over five decades in reaction rate. The resulting Arrhenius rate constant expression was

$$k = 5.3 \times 10^{15} \exp(-46.04/RT) \text{ s}^{-1},$$

with the activation energy in kcal/mol units. These data were compared with previous studies on AN/fuel mixtures.

The experimentally-determined ANFO parameters were incorporated into two models to investigate the potential for thermal runaway of 2,400 and 4,800 ton charges.

Overall, the work reported here showed ANFO to be a highly thermally stable energetic material, suitable for use in large conventional explosive charges. The data measured in this work allow predictions of minimum thermal runaway conditions for ANFO charges of various sizes and for various initial conditions. If the initial temperature of ANFO loaded into a container [e.g., a hemisphere of 2,400 tons (10 meters radius, 70 feet in diameter)] is near ambient, the models indicate that no credible external heating is likely to bring the material to a runaway condition. The remaining hazards are mainly from a large fire at the surface or inside the ANFO, or nearby in some other fuel, or from accidental detonation of some other explosive (e.g., a high explosive booster charge) near the ANFO.

Accession For	
NTIS CRA&I	<input checked="" type="checkbox"/>
DTIC TAB	<input type="checkbox"/>
Unannounced	<input type="checkbox"/>
Justification	
By	
Distribution /	
Availability Codes	
Dist	Avail and/or Special
A-1	

PREFACE

Part of the results reported here were supported by the Research Center for Energetic Materials. All of the data available on ANFO were combined to give a more complete picture.

The authors would like to thank Ken Bell of NMERI and Joe Renick of FCDNA for their encouragement and support. We also acknowledge Henric Ostmark and Nils Roman of the National Defence Research Establishment, Sundbyberg, Sweden, for supplying us with the PC version of TOPAZ, and Dr. Andrew Block-Bolten for measuring the melting characteristics of ANFO.

CONVERSION TABLE

Conversion factors for U.S. Customary to metric (SI) units of measurement.

MULTIPLY $\xrightarrow{\hspace{10em}}$ BY $\xrightarrow{\hspace{10em}}$ TO GET
 TO GET $\xleftarrow{\hspace{10em}}$ BY $\xleftarrow{\hspace{10em}}$ DIVIDE

angstrom	$1.000\ 000 \times E^{-10}$	meters (m)
atmosphere (normal)	$1.013\ 25 \times E^{+2}$	kilo pascal (kPa)
bar	$1.000\ 000 \times E^{+2}$	kilo pascal (kPa)
barn	$1.000\ 000 \times E^{-28}$	meter ² (m ²)
British thermal unit (thermochemical)	$1.054\ 350 \times E^{+3}$	joule (J)
calorie (thermochemical)	4.184 000	joule (J)
cal (thermochemical/cm ²)	$4.184\ 000 \times E^{-2}$	mega joule/m ² (MJ/m ²)
curie	$3.700\ 000 \times E^{+1}$	*giga becquerel (GBq)
degree (angle)	$1.745\ 329 \times E^{-2}$	radian (rad)
degree Fahrenheit	$t_k = (t^{\circ}F + 459.67)/1.8$	degree kelvin (K)
electron volt	$1.602\ 19 \times E^{-19}$	joule (J)
erg	$1.000\ 000 \times E^{-7}$	joule (J)
erg/second	$1.000\ 000 \times E^{-7}$	watt (W)
foot	$3.048\ 000 \times E^{-1}$	meter (m)
foot-pound-force	1.355 818	joule (J)
gallon (U.S. liquid)	$3.785\ 412 \times E^{-3}$	meter ³ (m ³)
inch	$2.540\ 000 \times E^{-2}$	meter (m)
jerk	$1.000\ 000 \times E^{+9}$	joule (J)
joule/kilogram (J/kg) radiation dose absorbed	1.000 000	Gray (Gy)
kilotons	4.183	terajoules
kip (1000 lbf)	$4.448\ 222 \times E^{+3}$	newton (N)
kip/inch ² (ksi)	$6.894\ 757 \times E^{+3}$	kilo pascal (kPa)
ktop	$1.000\ 000 \times E^{+2}$	newton-second/m ² (N-s/m ²)
micron	$1.000\ 000 \times E^{-6}$	meter (m)
mil	$2.540\ 000 \times E^{-5}$	meter (m)
mile (international)	$1.609\ 344 \times E^{+3}$	meter (m)
ounce	$2.834\ 952 \times E^{-2}$	kilogram (kg)
pound-force (lbs avoirdupois)	4.448 222	newton (N)
pound-force inch	$1.129\ 848 \times E^{-1}$	newton-meter (N·m)
pound-force/inch	$1.751\ 268 \times E^{+2}$	newton/meter (N/m)
pound-force/foot ²	$4.788\ 026 \times E^{-2}$	kilo pascal (kPa)
pound-force/inch ² (psi)	6.894 757	kilo pascal (kPa)
pound-mass (lbm avoirdupois)	$4.535\ 924 \times E^{-1}$	kilogram (kg)
pound-mass-foot ² (moment of inertia)	$4.214\ 011 \times E^{-2}$	kilogram-meter ² (kg·m ²)
pound-mass/foot ³	$1.601\ 846 \times E^{-1}$	kilogram/meter ³ (kg/m ³)
rad (radiation dose absorbed)	$1.000\ 000 \times E^{-2}$	**Gray (Gy)
roentgen	$2.579\ 760 \times E^{-4}$	coulomb/kilogram (C/kg)
shake	$1.000\ 000 \times E^{-8}$	second (s)
slug	$1.459\ 390 \times E^{+1}$	kilogram (kg)
torr (mm Hg, 0° C)	$1.333\ 22 \times E^{-1}$	kilo pascal (kPa)

*The becquerel (Bq) is the SI unit of radioactivity; 1 Bq = 1 event/s.
 **The Gray (GY) is the SI unit of absorbed radiation.

TABLE OF CONTENTS

Section	Page
SUMMARY	iii
PREFACE	iv
CONVERSION TABLE	v
FIGURES	viii
1 INTRODUCTION	1
2 BACKGROUND	2
2.1 THERMAL DECOMPOSITION KINETICS FROM COOK-OFF DATA	2
2.2 THERMAL EXPLOSION MODELS	2
2.3 SEMENOV MODEL	3
2.4 GENERAL PROPERTIES OF AN AND ANFO	4
2.5 DECOMPOSITION KINETICS OF AN/FUEL MIXTURES	4
2.6 OVERVIEW OF ANFO DATA	6
2.7 DECOMPOSITION OF AN	6
2.8 OVERVIEW OF AN DATA	8
3 EXPERIMENTAL	10
3.1 COOK-OFF TESTS	10
3.2 HENKIN-MCGILL TESTS	10
3.3 SSCB TESTS	10
3.4 1-LITER COOK-OFF TESTS	12
3.5 32-LITER COOK-OFF TESTS	12
3.6 TEST MATERIAL	15
4 RESULTS	16
4.1 DENSITIES AND MELTING POINT	16
4.2 HENKIN-MCGILL COOK-OFF DATA	16
4.3 SSCB COOK-OFF DATA	16
4.4 1-LITER COOK-OFF DATA	20
4.5 32-LITER COOK-OFF DATA	20
5 DATA ANALYSIS	25
5.1 THERMAL CONDUCTIVITY OF ANFO	25

5.2	KINETIC ANALYSIS	27
5.3	TOPAZ SIMULATIONS	27
5.4	APPLICATIONS TO LARGE CHARGES	31
5.5	F-K CALCULATIONS	31
5.6	TOPAZ CALCULATIONS	34
5.7	ANFO FIRE HAZARDS	34
6	CONCLUSIONS	36
7	REFERENCES	37
Appendix		
	Henkin Data for ANFO	A-1

LIST OF FIGURES

Figure	Page
2-1 AN phase characteristics	5
2-2 Arrhenius graph for AN/fuel mixtures	7
2-3 Arrhenius graph for AN	9
3-1 Schematic of SSCB cook-off apparatus	11
3-2 Schematic of 1-liter cook-off apparatus	13
3-3 Schematic of 32-liter cook-off apparatus	14
4-1 Henkin-McGill test data for ANFO	17
4-2 SSCB cook-off test #1 on ANFO	18
4-3 SSCB cook-off test #2 on ANFO	19
4-4 Temperature data for 32-liter cook-off test #2	22
4-5 32-liter cook-off data on expanded scale	23
4-6 32-liter cook-off data on expanded scale	24
5-1 Thermal conductivity fit to 1-liter cook-off data on ANFO	26
5-2 Arrhenius graph of ANFO decomposition data	28
5-3 Comparison of current and literature data on ANFO and AN	29
5-4 Calculated critical temperatures for ANFO cylinders	32
5-5 Calculated critical temperatures for large ANFO spheres	33

SECTION 1

INTRODUCTION

The explosive material used in the largest quantity per year in the world is ammonium nitrate (AN) mixed with a near stoichiometric amount (about 6 wt%) of hydrocarbon fuel oil (FO). Millions of pounds of this mixture, denoted ANFO, are produced each year and used for about 80 percent of all commercial blasting operations. The US consumption of ammonium nitrate based explosives was 4.0 billion pounds in 1991, accounting for 97 percent of all industrial explosives that were used. Large quantities of ANFO are therefore handled in manufacturing and transportation operations. The thermal stability and initiation insensitivity of ANFO are very high, making ANFO much safer to handle and store, especially when compared with previously used explosives such as dynamite. However, this high degree of safety may have contributed to a relaxation of handling precautions—possibly too large a relaxation.

The purpose of this study was to quantify the thermal hazards inherent in using large charges of ANFO in various DNA testing programs. For example, over the past several years ANFO charges from about 2400 to 4800 tons ($2.2 - 4.4 \times 10^6$ kg) have been used to simulate the environments caused by nuclear weapons. In hemispherical shapes, these weights represent quantities of ANFO with radii of 1070 and 1350 cm (70 and 88 foot diameters). The main question addressed in this work was whether it is possible for ANFO charges of this size to self-heat as a result of chemical decomposition heat which cannot be conducted away as fast as it is generated.

SECTION 2

BACKGROUND

2.1 THERMAL DECOMPOSITION KINETICS FROM COOK-OFF DATA.

Thermal methods of measuring reaction rates rely on the heat produced (or absorbed) by a system as a measure of the amount of reaction. We have utilized thermal runaway (isothermal cook-off) tests on ANFO to determine critical temperatures (i.e., minimum temperatures for runaway self-heating) from which we have derived steady-state global reaction rates. Since different sample sizes yield different critical temperatures (i.e., different rates of reaction), we have been able to determine the global rate constant parameters for ANFO decomposition over a range of over five decades.

Thermal runaway from exothermic reactions is possible for many chemicals and energetic materials. This happens when the rate of heat generation from chemical decomposition exceeds the rate of heat loss from the material. At the critical temperature, these two rates are equal. Quantitatively describing the rate of heat loss by conduction from simple sample configurations is a relatively straightforward problem; once the problem is solved, the rate of heat generation can be determined.

Since the rate of heat generation is the product of the reaction rate and the heat of reaction, the reaction rate can be determined if the heat of reaction is known. Cook-off tests on samples of approximately 25 kg or so yield rate constant determinations in the 10^{-8} s^{-1} range, whereas tests on smaller samples yield rate data at much higher values, about 10^{-6} and 10^{-2} s^{-1} for 1 kg and 40 mg samples, respectively. The corresponding rate constant at the critical temperature for approximately 2,000 tons would be in the 10^{-11} s^{-1} range.

2.2 THERMAL EXPLOSION MODELS.

The theory of thermal ignition has been treated by many workers, including Zeldovitch, et al.¹ (1939), Frank-Kamenetskii² (1939), Gray and Lee³ (1968), Zinn and Mader⁴ (1960), Zinn and Rogers⁵ (1962), and many others. For solid explosives, consideration can be confined to conductive heat losses [i.e., the well-known Frank-Kamenetskii (F-K) model]. The assumptions and limitations of this model have been discussed by the authors listed above. In the case of symmetric configurations, the F-K formula gives the critical temperature (T_c , K) as

$$T_c = \frac{E_a / R}{\ln \left[\frac{r^2 \rho Q A E_a}{T_c^2 \lambda S h R} \right]}$$

where

T_c	=	Critical temperature, K
E_a	=	Activation energy, cal/mol
A	=	Preexponential factor, s^{-1}
R	=	Gas constant, 1.987 cal/K/mol
r	=	Radius or half-thickness, cm
ρ	=	Density, g/cm^3

- Q = Heat of decomposition reaction, cal/g
 λ = Thermal conductivity, cal/cm/s/K
 Sh = Shape factor, 3.32 for sphere, 2.0 for infinite cylinder, 0.88 for slab, 2.5 for cylinder with length approximately equal to diameter

The main unknowns in the F-K analysis are the thermal conductivity, the heat of reaction, and the Arrhenius rate constant parameters, A and E_a , which give the rate constant (k) value at any temperature as $k = A \exp(-E_a/RT)$. The density, radius, and shape factor are usually known. If all these parameters are known, accurate predictions of critical temperatures can often be made (when the situation fits the assumptions of the F-K model).

Conversely, if the critical temperature is experimentally measured and the thermal conductivity is known, combinations of A and E_a can be determined which satisfy the F-K formula. It is found that if E_a is estimated and the A -factor is determined, the resulting value of k is only slightly dependent upon the value of E_a used. Thus we can determine a value for k at the temperature T_c by measuring the critical temperature of an explosive in a given sample size and shape.

Other rate constant values at different temperatures can be determined by measuring critical temperatures for other sample sizes. A fit to these $k(T_c)$ data points vs. $1/T$ yields a global rate coefficient which will describe cook-off behavior for this explosive over a wide range of conditions.

2.3 SEMENOV MODEL.

For containers of hot stirred liquids, the temperature profile from the edge to the center of the material will not show the expected variation appropriate to the F-K model of heat losses only by conduction. The situation of a well stirred material with an almost constant temperature profile across the material is described by the Semenov model⁶ according to the equation

$$V Q \rho A \exp(-E_a/(R T_c)) = \alpha SA T_c^2 / E_a ,$$

where

- V = Volume of explosive, cm^3
 Q = Heat of decomposition reaction, cal/g
 ρ = Density, g/cm^3
 A = Preexponential factor, s^{-1}
 E_a = Activation energy, cal/mol
 R = Gas constant, cal/K/mol
 T_c = Critical temperature, K
 α = Heat transfer coefficient of wall, $\text{cal}/(\text{cm}^2 \text{ s K})$
 SA = Surface Area, cm^2

In this model, the same values for the kinetic factors, density, and heat of decomposition would be used as in the F-K model. The surface area and volume would be characteristic of a specific explosive sample and would be known. The remaining unknown is the overall heat transfer coefficient, α . The work of Rogers, Guiana, and Loverro⁷ discuss values for α ranging from 0.0085 for an aluminum wall to 0.0022 for a steel wall.

2.4 GENERAL PROPERTIES OF AN AND ANFO⁸.

Crystalline ammonium nitrate absorbs water from the air and forms hard cakes which makes it difficult to handle (e.g., spreading as a fertilizer). These handling difficulties led to the manufacture of prilled AN (i.e., small—approximately 2 mm diameter—balls of AN created by spraying AN solution in a drying tower). After about 1945, the residual moisture content of the prills was allowed to increase, producing a higher porosity AN denoted as fuel-grade ammonium nitrate (FGAN). The previously used low porosity AN was called explosive-grade ammonium nitrate. The available porosity in FGAN of about 0.07 cm³/g is almost exactly the amount needed to absorb the quantity of oil to yield an oxygen balanced (stoichiometrically balanced to CO₂ and H₂O reaction products) ANFO product. The AN prills also contain unavailable porosity (i.e., not available to absorb oil) which is also important in giving the ANFO a low final density and in sensitizing it to shock initiation.

AN has several solid state phases over the temperature range of interest. This complicates its use in applications where expansion may cause difficulties. These phases and some of their characteristics are summarized in Figure 2-1. Of special interest are the expansions and heats of transition that occur at the IV to III transition at 32.3°C, the III to II transition at 84.2°C, and the II to I transition at 125.2°C before melting at about 169°C.

The explosive characteristics of FGAN became widely recognized after the explosion of a shipload of over 3,000 tons at Texas City in 1947. The specific product that exploded was FGAN coated with about 1 percent wax for anti-caking purposes. (Actually the "wax" was a mixture of paraffin, rosin, and petrolatum.) However, this mixture is more sensitive than either pure AN or the oxygen balanced mixture with 5.5 percent wax. The explosion was caused by several factors: the relatively high sensitivity of the wax-coated FGAN; the large charge size; the high initial temperature, about 32°C; and the paper bags in which the material was shipped. It is likely that the paper-AN combination exhibited a lower thermal stability than the FGAN itself and it self-heated, possibly starting the fires that ultimately lead to detonation of the whole shipload of FGAN. Following the Texas City incident, the anti-caking wax coating was replaced by a coating of kieselguhr.

2.5 DECOMPOSITION KINETICS OF AN/FUEL MIXTURES.

Although the literature on the thermal stability of AN is extensive, few studies have been performed on ANFO. A review of the studies of AN/hydrocarbon mixtures is given below with a brief overview of the work on AN.

Hainer⁹ studied the thermal decomposition of AN and 3 percent wax-coated fertilizer grade AN (FGAN) using weight loss and N₂O evolution measurements over the temperature range 220-290°C for AN and 70-230°C for FGAN. At the lower temperatures, samples as large as 100 pounds were used for gas evolution measurements, resulting in rate constant determinations as small as 3 x 10⁻⁹ s⁻¹ at 132°C for AN and 2-10 x 10⁻¹² s⁻¹ at 70°C for FGAN. No other measurements at these low reaction rates are available for either material.

Hainer's kinetic results (E_a in kcal/mol units) for FGAN are

$$k = 3.7 \times 10^{10} \exp(-34.8/RT) \text{ s}^{-1}.$$

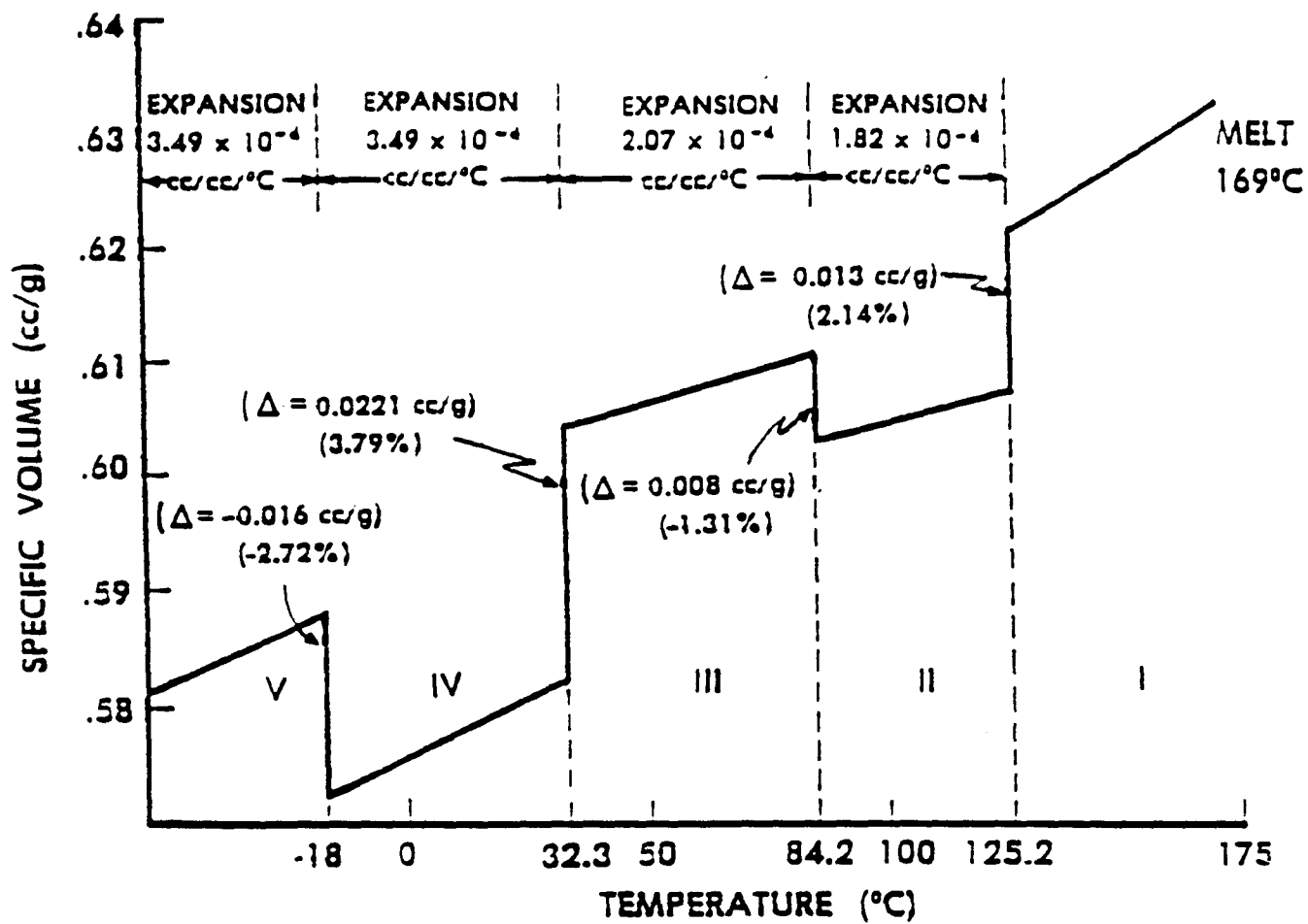


Figure 2-1. Ammonium nitrate phase characteristics.

Hainer concluded that the reaction rates of AN and FGAN were similar at high temperatures (>200°C), but that of FGAN was much larger at low temperatures (by about 100 times at 100°C). However, we noted that the rate constant for AN at low temperatures that Hainer used for comparison was extrapolated over many decades using an uncertain activation energy.

Oxley, Kaushik, and Gilson¹⁰ studied AN, emulsion, and AN mixed with 5 wt% mineral oil (denoted ANMO to differentiate it from commercial ANFO) by isothermally decomposing the test material sealed in glass tubes and by using DSC techniques. ANMO reacted slightly faster than neat AN at temperatures higher than about 270°C. However, at lower temperatures, the ANMO reaction was faster than AN only for the initial part (40 percent at 270°C, decreasing to 14 percent at 230°C) of the decomposition. Kinetic parameters were determined for both the more rapid initial (denoted "early") and the slower final (denoted "late") portions of the total reaction. The early kinetics of ANMO decomposition were characterized over the temperature range 230-370°C by

$$k = 2.4 \times 10^{11} \exp(-35.2/RT) \text{ s}^{-1}.$$

2.6 OVERVIEW OF ANFO DATA.

The kinetic data for the two studies of AN/fuel are plotted in Arrhenius form in Figure 2-2 for comparison. The activation energies of the two expressions are similar, with the two lines offset from each other by about a decade.

2.7 DECOMPOSITION OF AN.

Extensive literature exists on AN decomposition, including information on kinetics, mechanisms, catalyst, and product composition. King and Bauer¹¹ at Queens University, Ontario, reviewed the literature on AN and published a series of twelve reports. Number four of this series covers thermal decomposition mechanisms and kinetics up to 1974. Report number one covers accidents with AN and number nine covers the deflagration to detonation transition in molten AN.

Robertson¹² studied isothermal AN decomposition by pressure measurements over the temperature range 243-361°C. This work extended to higher temperatures than are typical. The results were fit into the Arrhenius expression

$$k = 6.3 \times 10^{13} \exp(-40.5/RT) \text{ s}^{-1},$$

with an estimated uncertainty of ± 2.5 kcal/mol in the activation energy. These rate constant results are higher than reported in most other work done in this temperature range.

Hainer's kinetic results for AN (220-290°C) from the same study⁹ as discussed above were

$$k = 8.4 \times 10^{18} \exp(-55.6/RT) \text{ s}^{-1}.$$

It should be noted that these data for AN did not cover as extensive a temperature range as for the FGAN data.

Cook and Abegg¹³ studied AN decomposition using real time weight loss measurements over the

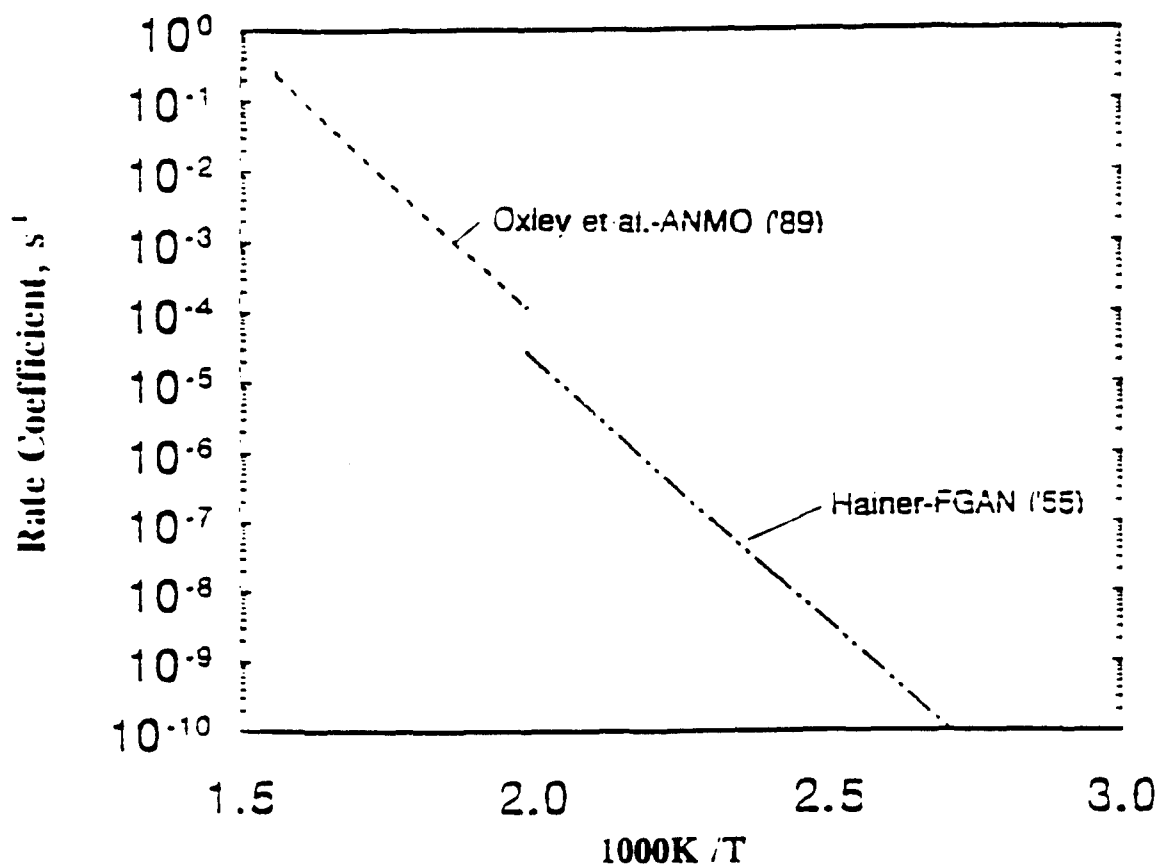


Figure 2-2. Arrhenius graph of literature data on AN/fuel mixtures.

temperature range 218-267°C. First order behavior was observed in all experiments, with no autocatalysis. Their rate constant was

$$k = 1.9 \times 10^{12} \exp(-38.3/RT) \text{ s}^{-1} .$$

Cook and Abegg's expression was corrected for AN vaporization by King and Bauer¹¹ to give

$$k = 4.9 \times 10^{11} \exp(-37.0/RT) \text{ s}^{-1} .$$

Keenan and Dimitriadis¹⁴ used a gas evolution method to study the decomposition of AN from 230-265°C. Their results gave

$$k = 3.0 \times 10^{16} \exp(-49.5/RT) \text{ s}^{-1} .$$

Rosser, Inami, and Wise¹⁵ studied AN decomposition from 225-275°C using N₂O evolution rates in a flow system. By seeding the inlet gas flow, they showed clearly that NH₃ and H₂O inhibit AN decomposition, and HNO₃ promotes AN decomposition; thus the overall rate of decomposition depends on the gas composition in contact with the AN. Their nominal rate constant was

$$k = 1.8 \times 10^{13} \exp(-41.0/RT) \text{ s}^{-1} .$$

Brower, Oxley, and Tewari¹⁶ calculated rate constants for AN decomposition in sealed glass tubes from total gas evolution and nitrogen fraction measurements over the temperature range 200-380°C. Their data were fit to separate high and low temperature expressions

$$k = 8.5 \times 10^{14} \exp(-46.3/RT) \text{ s}^{-1} \text{ (high temperature), and}$$

$$k = 1.3 \times 10^8 \exp(-28.2/RT) \text{ s}^{-1} \text{ (low temperature).}$$

2.8 OVERVIEW OF AN DATA.

The kinetic data for AN are plotted in Arrhenius form in Figure 2-3 for comparison. Although all of these rate constant expressions are derived from data which agree fairly well (within a factor of ten) in the temperature region of overlap, they were almost all measured at relatively high temperatures. If these expressions are extrapolated to the lower temperatures, which are of interest for storage stability considerations for large quantities of AN or ANFO, the disagreement is much larger.

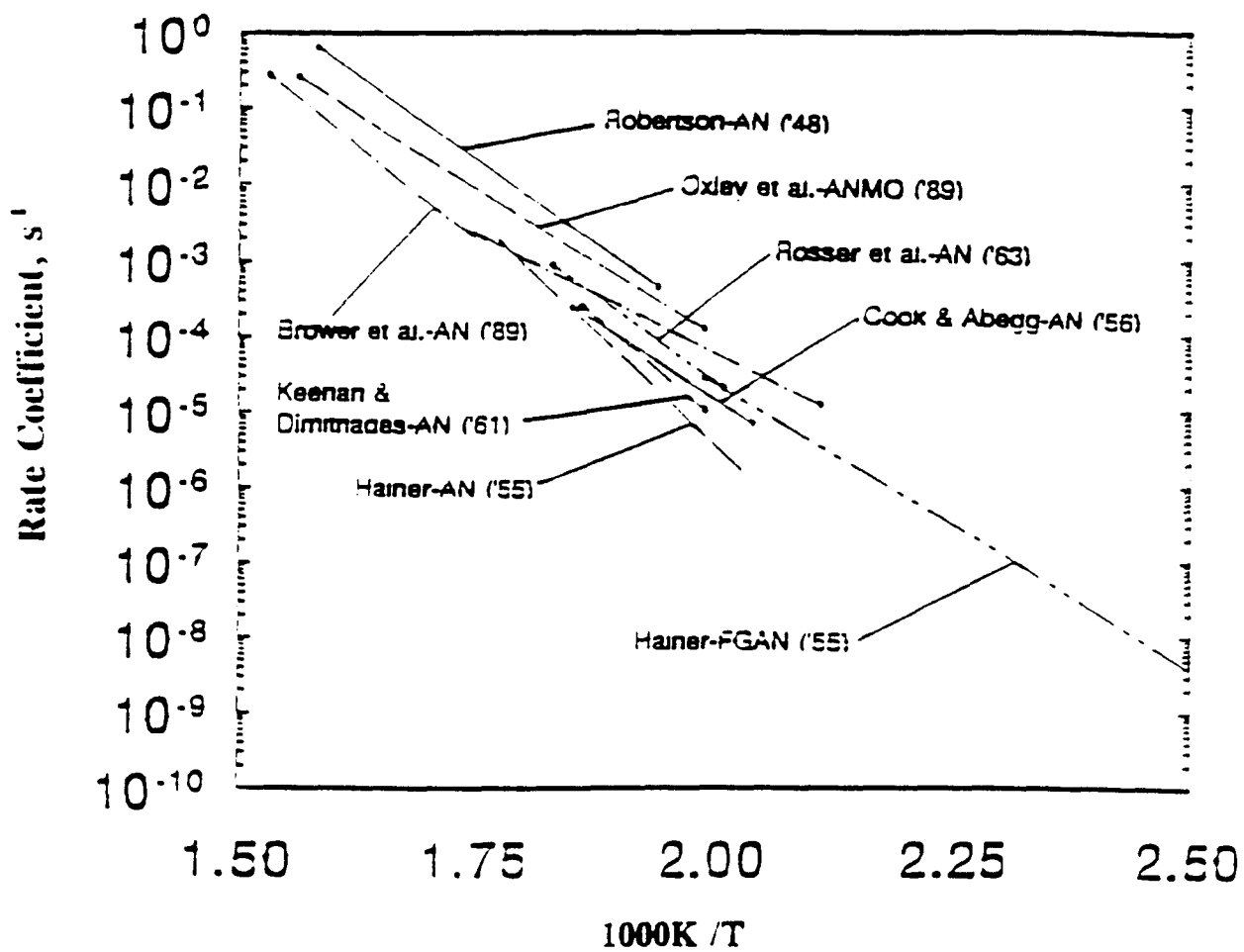


Figure 2-3. Arrhenius graph of literature data on AN.

SECTION 3

EXPERIMENTAL

3.1 COOK-OFF TESTS.

The critical temperature, T_c (i.e., the lowest temperature at which an explosive sample exhibits thermal runaway from chemical self-heating) was determined for three different sample sizes of ANFO.

3.2 HENKIN-MCGILL TESTS.

The Henkin-McGill test¹⁷ is the smallest thermal runaway test. It has the advantage of being small enough, using samples of less than 0.1 g, to be run in the laboratory environment using an apparatus similar to those described by Rogers.¹⁸

Ground ANFO samples were sealed inside standard aluminum blasting-cap shells using a hand-operated hydraulic press and specially made hollow aluminum plugs. A two-step pressing procedure was used to compress the sample and then to expand the wall of the plug to create a seal with the shell. This gave the sample a reproducible geometry of a disc (0.65 cm diameter with an average thickness of 0.071 cm) so it could be considered to be an infinite slab for analysis (with shape factor = 0.88). A micrometer was used to measure the thickness of each disc.

The temperature of the Wood's metal bath was controlled by an Omega Engineering, Inc. Model 920 proportional controller. The actual bath temperature was measured immediately prior to each test using an Omega K-type stainless steel sheathed thermocouple and a Fluke model 52 digital thermometer readout. The sample was lowered into the hot bath in a remote operation using a compressed air-driven piston/cylinder. The time-to-explosion was measured using a digital stopwatch from the initial time when the sample was immersed in the molten metal bath to the time, if any, at which the sample holder ruptured. The timing uncertainty was estimated to be about plus or minus one second. To find the critical temperature, the time-to-explosion tests were repeated at various temperatures until the minimum temperature was found at which thermal runaway and shell rupture occurred.

3.3 SSCB TESTS.

Pakulak and Cragin¹⁹ developed a small cook-off test, called the super small cook-off bomb (SSCB) test, using a 5/8 inch (1.6 cm) i.d. tube with witness plates bolted directly to the open ends of the tube to contain the explosive. In the work reported here, a modified SSCB apparatus, based loosely on the Navy test, was used. Thick-walled aluminum tubing with 2.5 cm o.d. and 1.6 cm i.d. was threaded and sealed using stainless steel pipe caps on each end. A 1/16 inch (0.16 cm) diameter stainless steel sheathed thermocouple was installed through the bottom end cap using a Swagelok fitting to measure the axial sample temperature. A diagram of the apparatus is shown in Figure 3-1. The assembled tube containing the explosive was heated by contact with a split and spring-loaded 4 inch (10 cm) diameter brass platen containing four embedded 250 Watt electric cartridge heaters. Heating time from

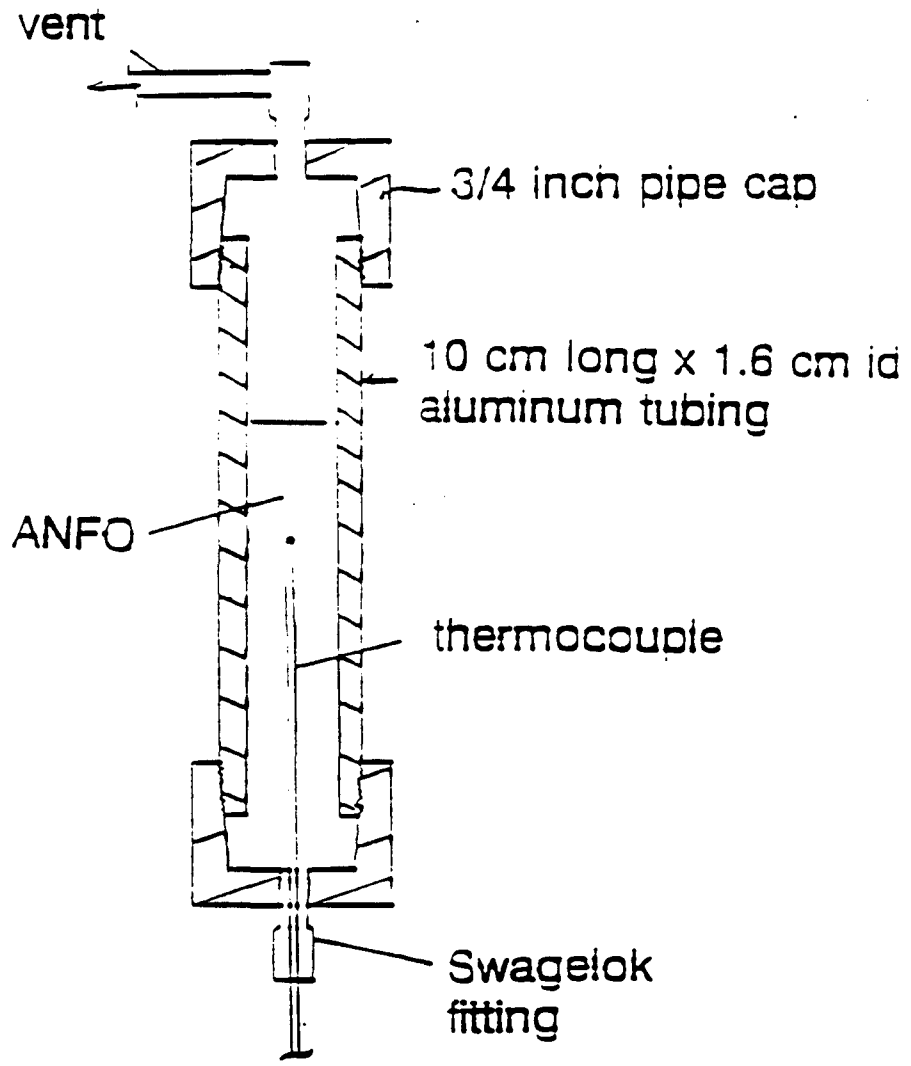


Figure 3-1. Schematic of SSCB cook-off apparatus.

ambient was about 10 minutes. The tests reported here were run vented to the atmosphere.

The thermocouple located inside the test vessel and the two thermocouples located in the platen were connected to a Hewlett-Packard Vectra personal computer using an Omega Engineering, Inc. White Box interface card and software. The software was programmed to record the temperatures at one-minute intervals. The data acquisition board was checked prior to each test using a precision voltage source thermocouple calibrator. The channels typically agreed within $\pm 0.1^{\circ}\text{C}$. The desired platen temperature was also programmed into the Omega software which then controlled a solid-state relay connected to the electric heaters. ASCII data files were imported into a Quattro Pro spreadsheet for data analysis and plotting.

3.4 1-LITER COOK-OFF TESTS.

Charges of about 0.8 kg of ANFO were tested using glass round-bottomed flasks as charge containers using three 0.16 cm diameter stainless steel sheathed thermocouples located at the sample center, mid-radius, and wall. The sample was heated using a stirred hot oil bath using Dow Corning 200 heat transfer fluid, as shown in Figure 3-2. Another thermocouple was inserted into the oil bath to monitor its temperature. A two-bladed stirrer was used to obtain uniform oil temperature. The same data acquisition and data reduction methods used for the SSCB tests were used here.

3.5 32-LITER COOK-OFF TESTS.

Larger quantities of ANFO were used to perform thermal runaway tests on the material at temperatures below the melting point ($165\text{-}169^{\circ}\text{C}$). To minimize fragments should the charge detonate, a test vessel was fabricated based on a 32-liter, heavy-walled glass battery jar (41 cm diameter, 31 cm deep) with a lightweight aluminum lid. Silicone rubber-insulated, flexible electric heating bands were used on the top, bottom, and sides of the vessel for heating. Insulating blanket material was also wrapped around, over, and under the vessel.

Three 0.16 cm diameter thermocouples were located in the charge as shown in Figure 3-3. The thermocouple signals were connected to voltage-to-current modules (Omega Engineering, OM3 modules) using eight-pair K-type thermocouple wire cable to transmit the signals over approximately 210 meters (600 feet) of shielded multi-pair cable to the instrumentation bunker. These tests utilized the same type of computer and interface board that were used for recording the data and controlling the heaters for the SSCB and 1-liter tests. The analog-to-digital board was reprogrammed from direct processing of thermocouple voltage inputs to processing of 20 milliampere current loop signals. Remote control software (Close-Up) and high-speed modems (Hayes Optima 9600) were installed on the computer located at the cook-off site (used to control the test temperature and record the data), as well as on computers used for remote monitoring of the test progress.

The absolute calibration of the thermocouples and voltage-to-current modules were checked using a voltage source calibrator just prior to beginning the test. Slight linear offsets were applied to the various thermocouple signals in the data acquisition program to bring them into agreement within $\pm 0.5^{\circ}\text{C}$.

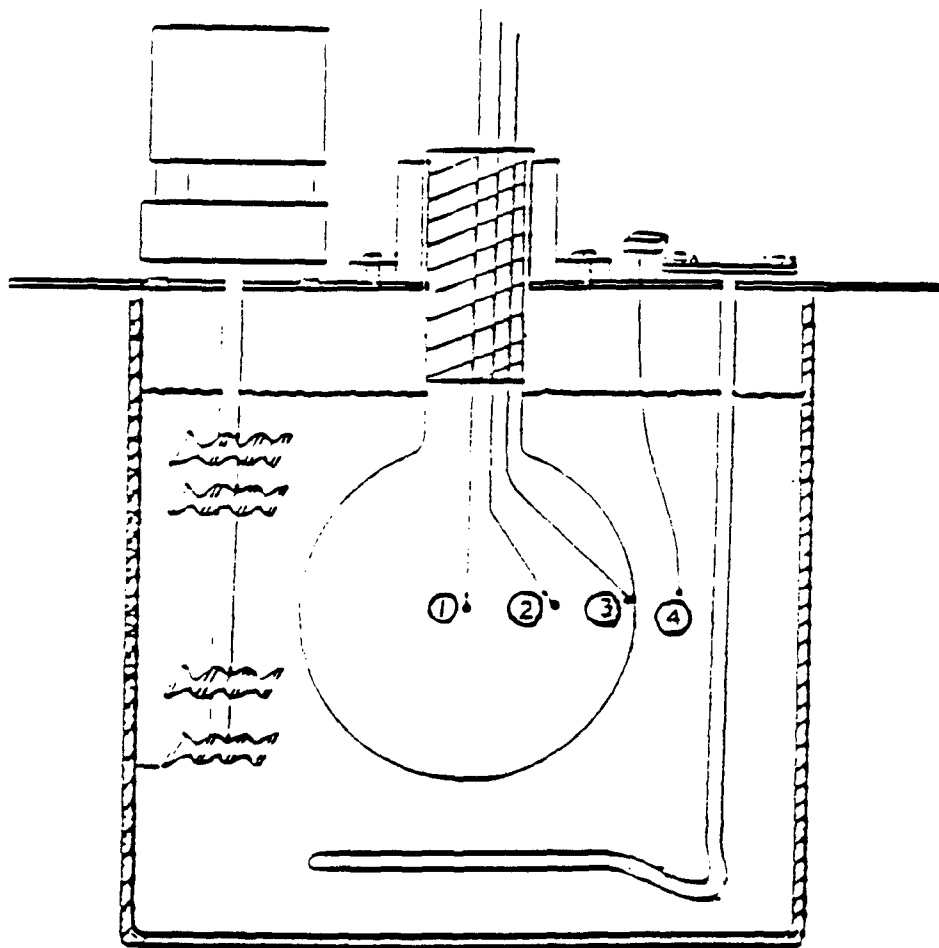


Figure 3-2. Schematic of 1-liter cook-off apparatus.

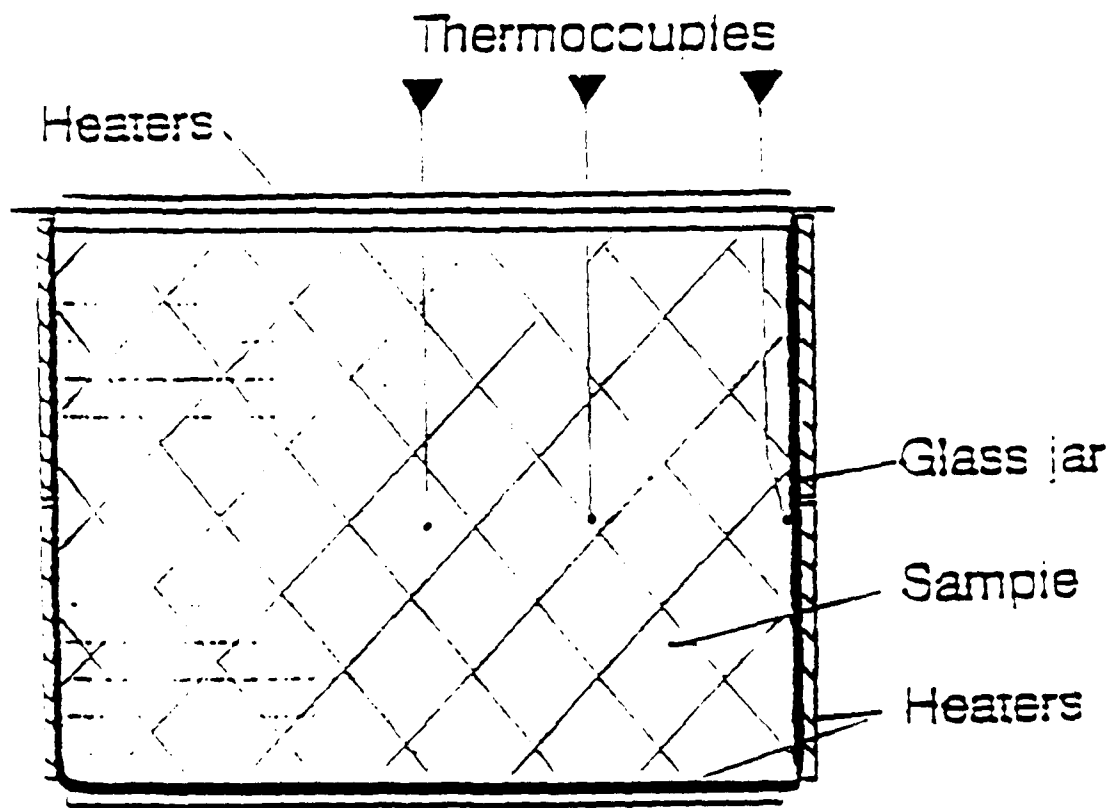


Figure 3-3. Schematic of 32-liter cook-off apparatus.

A plywood box was placed over the whole apparatus to provide protection from weather. These tests were performed at the remote EMRTC Fast/Slow Cook-off site which is rated for large explosive charges and has continuous video surveillance for security.

3.6 TEST MATERIAL.

Commercial ANFO obtained from ICI Explosives in Albuquerque was used for all tests. The ANFO was used as received except for grinding it for Henkin-McGill tests (where the prills were too large).

SECTION 4

RESULTS

4.1 DENSITIES AND MELTING POINT.

The density of the ANFO was measured four times using a cup of known volume and a precision balance. The results were an ANFO density of $0.85 \pm 0.01 \text{ g/cm}^3$. The average density of the Henkin-McGill samples which were pressed into the shells for testing was measured in place as about 1.65 g/cm^3 .

The melting temperature of this ANFO was measured using about 2 grams of material inside a test tube heated by an oil bath. Some melting (wetting) was observed at 160°C , but melting was not complete until about 170°C . Melting tests were also performed using a Mettler hot stage with microscopic observation. No melting was observed below 167.6°C , with flooding observed by 169.6°C . The melting point is thus between 167 and 169°C .

4.2 HENKIN-MCGILL COOK-OFF DATA.

About twenty-five $40 \pm 1 \text{ mg}$ samples were tested to determine the small-scale critical temperature. These samples had an average thickness of 0.071 cm. The experimental data are listed in Table 1 (Attachment 1) and shown in Figure 4-1 (go's and no-go's are denoted by open and filled symbols, respectively). Little overlap was found between the go's and no-go's near the critical temperature. The definition of the critical temperature is the temperature for the lowest go, ignoring that there may be some no-go's at higher temperatures. Thus the critical temperature for this sample size of ANFO was determined to be 297°C . The positive tests were characterized by relatively weak events.

4.3 SSCB COOK-OFF DATA.

Two SSCB tests were run on approximately 25 g samples of ANFO in 1.6 cm diameter aluminum cylinders at temperatures above the melting temperature. These tests were tried with the hope that the small cross-section of this vessel would prevent convection in the liquid ANFO. The results of the first SSCB test at 230°C are shown in Figure 4-2. The test temperature was reached in about 14 minutes. After about 37 minutes, a rise in sample temperature is shown, followed by a temperature decrease. Although this change in temperature appears relatively minor, visual monitoring of the test apparatus via a video camera showed that a short length of steel tubing connected to the vent fitting of the vessel had been ejected. Smoke and particles escaped from the vent following this time, indicating that a cook-off had occurred. The decrease in temperature was thought to be caused by ejection of a significant amount of the liquid ANFO, exposing the tip of the thermocouple and leading to lower temperature measurements.

The second SSCB test was run at a test temperature of 221°C , as shown in Figure 4-3 on the following page, for about 180 minutes, followed by an additional 1600 minutes at 225°C . No

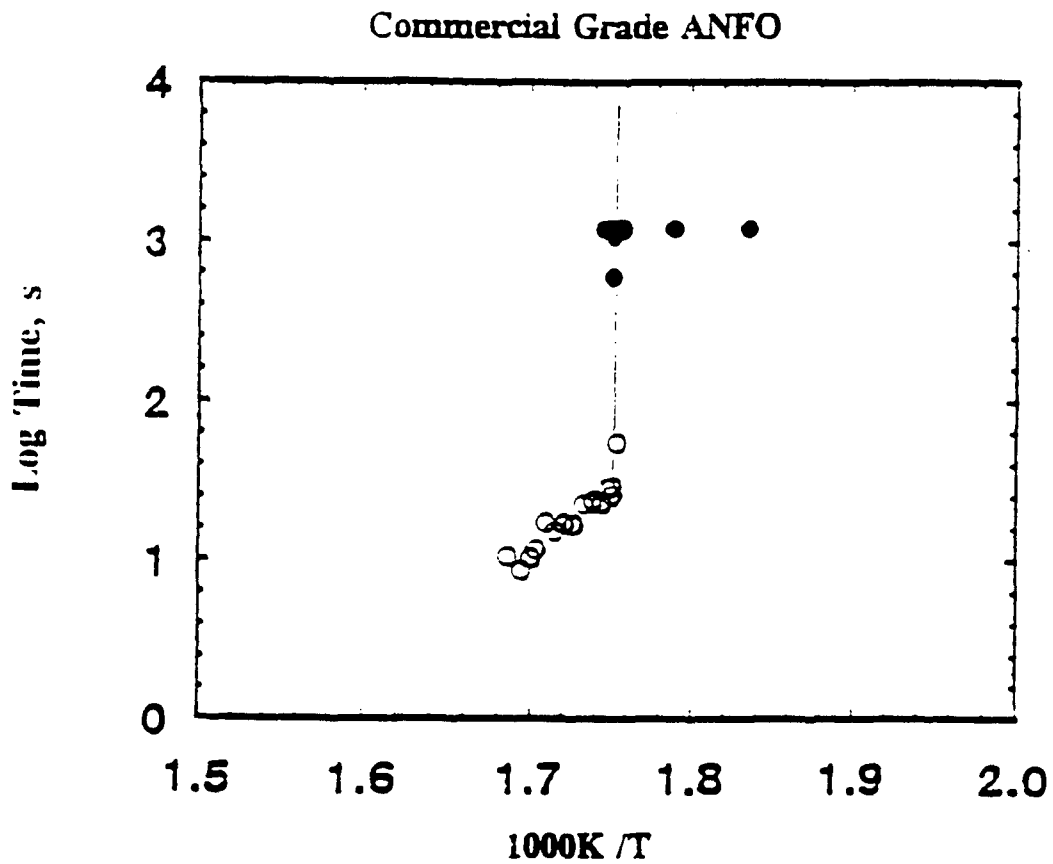


Figure 4-1. Henkin-McGill data for 40 mg cook-off tests on commercial ANFO. The filled symbols represent no-go results and the open symbols represent go's. The critical temperature was found to be 297°C.

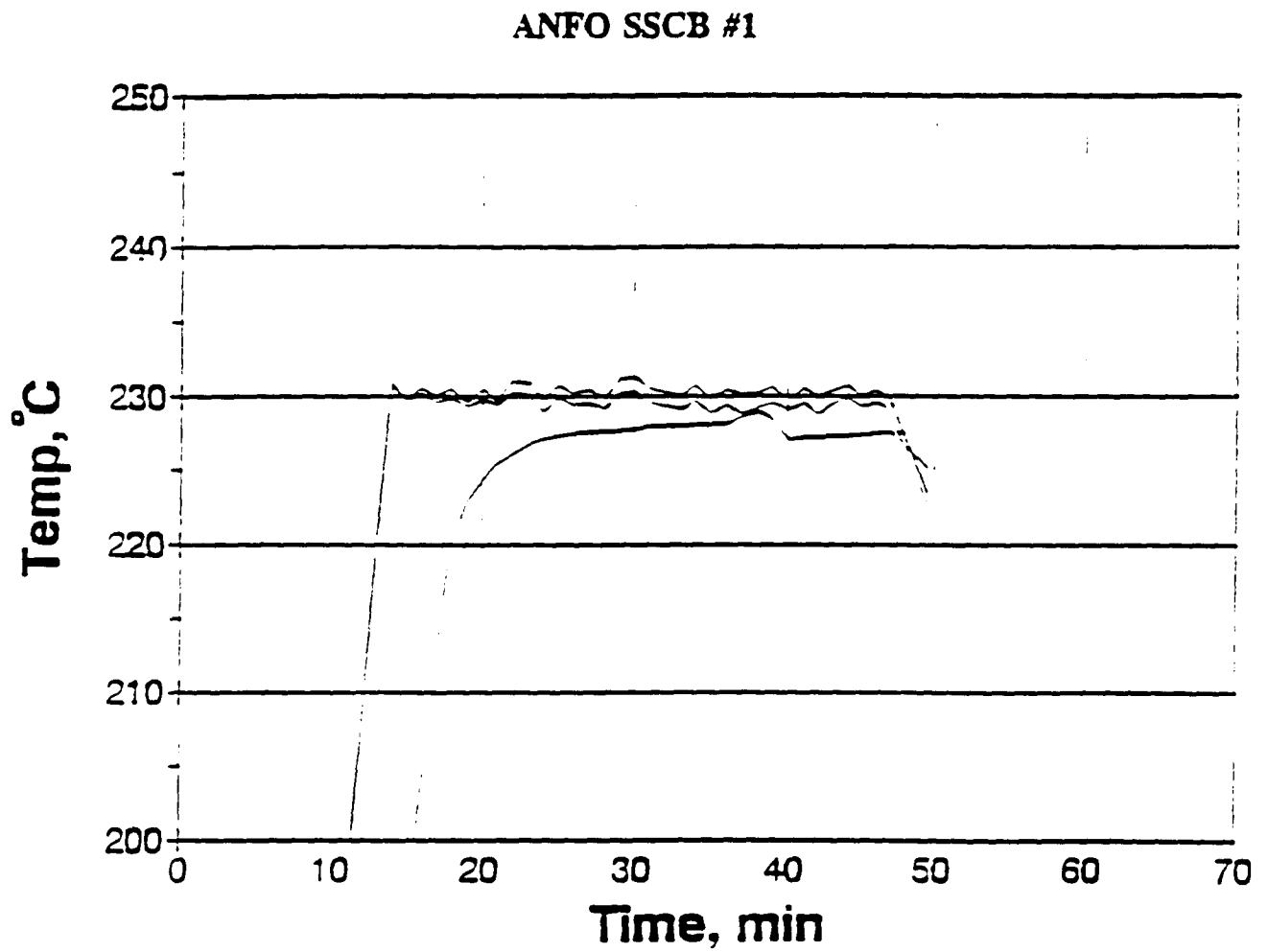


Figure 4-2. SSCB cook-off test #1 for ANFO. An event occurred at about 38 minutes at 230°C.

ANFO SSCB #2

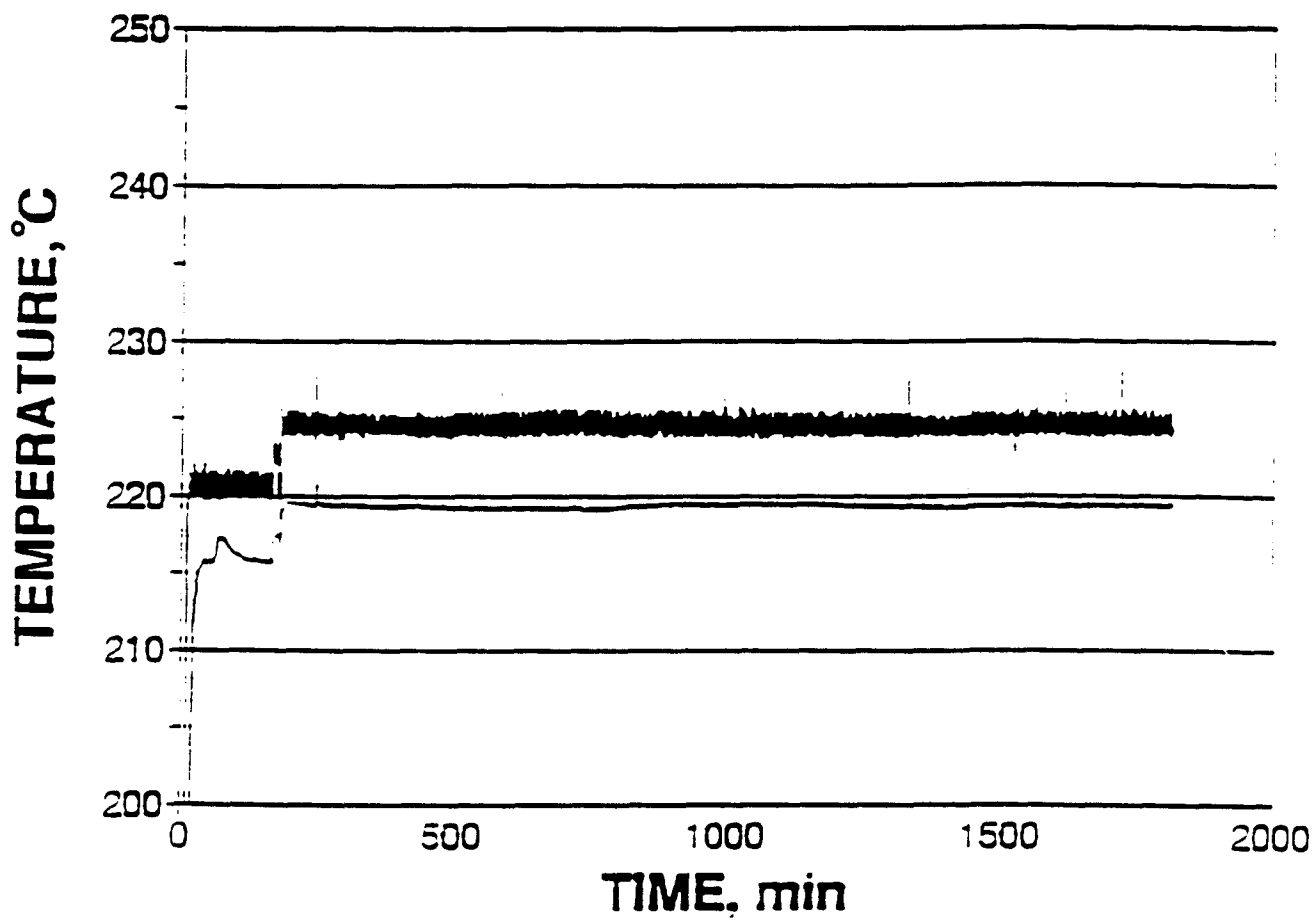


Figure 4-3. SSCB cook-off test #2 for ANFO. No thermal runaway was observed at 225°C.

chemical self-heating was observed.

The conclusion reached was that the critical temperature for this sample size of ANFO was between 221 and 230°C, about 225°C.

4.4 1-LITER COOK-OFF DATA.

One-liter isothermal cook-off tests were run²⁰ at 160, 163, 180, and 205°C without observing thermal runaway. However, visual monitoring of the tests showed that considerable gas evolution was occurring during the test, with resulting vigorous stirring of the molten ANFO at temperatures above 170°C. This prevented thermal runaway at the expected temperature (approximately 180-190°C).

The Frank-Kamenetskii (F-K) model assumes that heat loss is only by conduction processes. The enhanced heat transfer from stirring the explosive changes the situation and makes the F-K model no longer applicable. The experimental cook-off test data are still valid, but predictions and analysis using the F-K model are not applicable.

Approximate Semenov calculations were performed to estimate the critical temperature for a well-stirred 1-liter test sample of ANFO. These calculations require, in addition to parameters used in the F-K model, a value for the overall heat transfer coefficient at the wall of the container. This value is not precisely known. However, for the expected range of the heat transfer coefficient, Semenov calculations yielded critical temperatures for molten ANFO in the 216-233°C range. Since this temperature range is higher than where any of the cook-off tests were performed, the calculation supports the hypothesis that stirring the sample from the bubbling phase prevented runaway under our experimental conditions.

Because the primary interest was in solid ANFO and due to uncertainties in analyzing the data, additional 1-liter tests were not performed at higher temperatures.

4.5 32-LITER COOK-OFF DATA.

The first 32-liter cook-off test was performed using about 25 kg (55 pounds) of ANFO. In comparison with the smaller tests, the distance between the charge and the data acquisition was much greater in this case, about 210 meters (600 feet). This required electronic line drivers to send the thermocouple signals over long cables. The cook-off test was initiated at a wall temperature of 145°C. At about 4.1 days into this first large ANFO test, the apparatus suffered a near-hit from a lightning strike, and all of the control electronics were destroyed. When power was returned to the apparatus, shorted heater relays caused a fire. The ANFO burned slowly without incident.

The second 32-liter test setup was identical to the ill-fated first test. The initial wall temperature was set to 151°C. The ANFO, being a good thermal insulator, required about four days to reach the test temperature throughout the charge, as shown on the temperature

profiles in Figure 4-4. No heat generation was observed during this period, so the wall temperature was increased to 158°C at a test time of 5.2 days, as shown in more detail in Figure 4-5. The charge was held under these conditions for about 2.5 days, during which the ANFO temperature gradually increased, but no self-heating was observed. The charge temperature again increased, this time to 162°C, just below the melting temperature of ANFO. The test was continued for another 2.1 days (from 7.7 to 9.8 days) without incident. The temperature was then increased to 165°C for about 0.8 day, and finally set to 175°C.

The final two days of the test are shown in Figure 4-6 on expanded scales. The mid-radius thermocouple signal was lost at about 9.2 days into the test (due to a thermocouple voltage-to-current module failure, again from lightening in the area). Not all of the details of the temperature profiles are understood. Upon increasing the wall temperature from 165 to 175°C, the center temperature signal began to increase and then showed an abrupt rapid increase when that temperature was 168°C. The ANFO temperature near the wall would have been slightly hotter. A rapid runaway reaction occurred which ignited the ANFO. Examination of the test vessel showed that about 90 percent of the ANFO burned, leaving a fused layer about 3-4 cm thick in the bottom of the vessel. The critical temperature for this test was concluded to be about 168±5°C.

32-Liter ANFO Cook-off #2

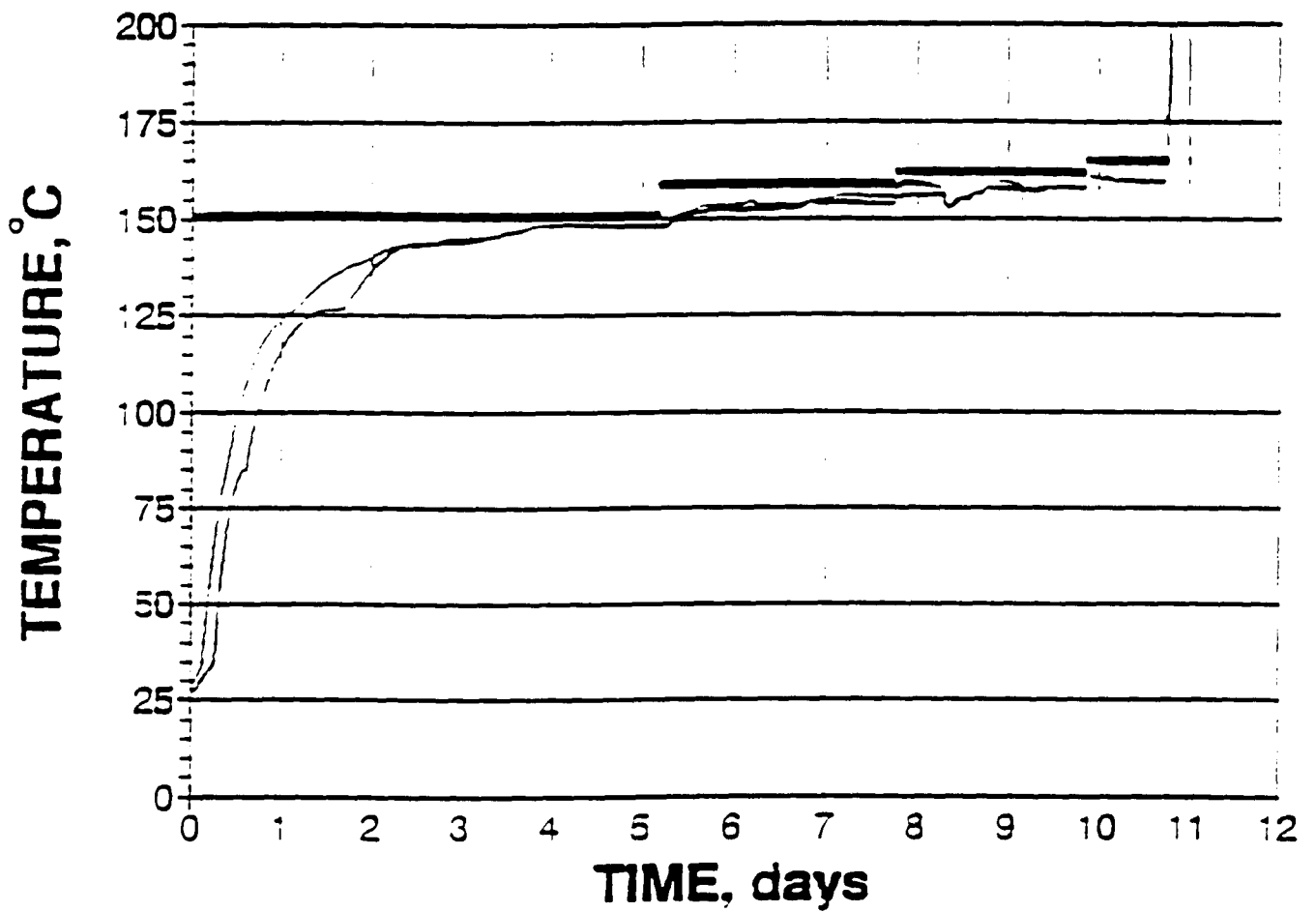


Figure 4-4. Temperature data for 32-liter cook-off test #2.

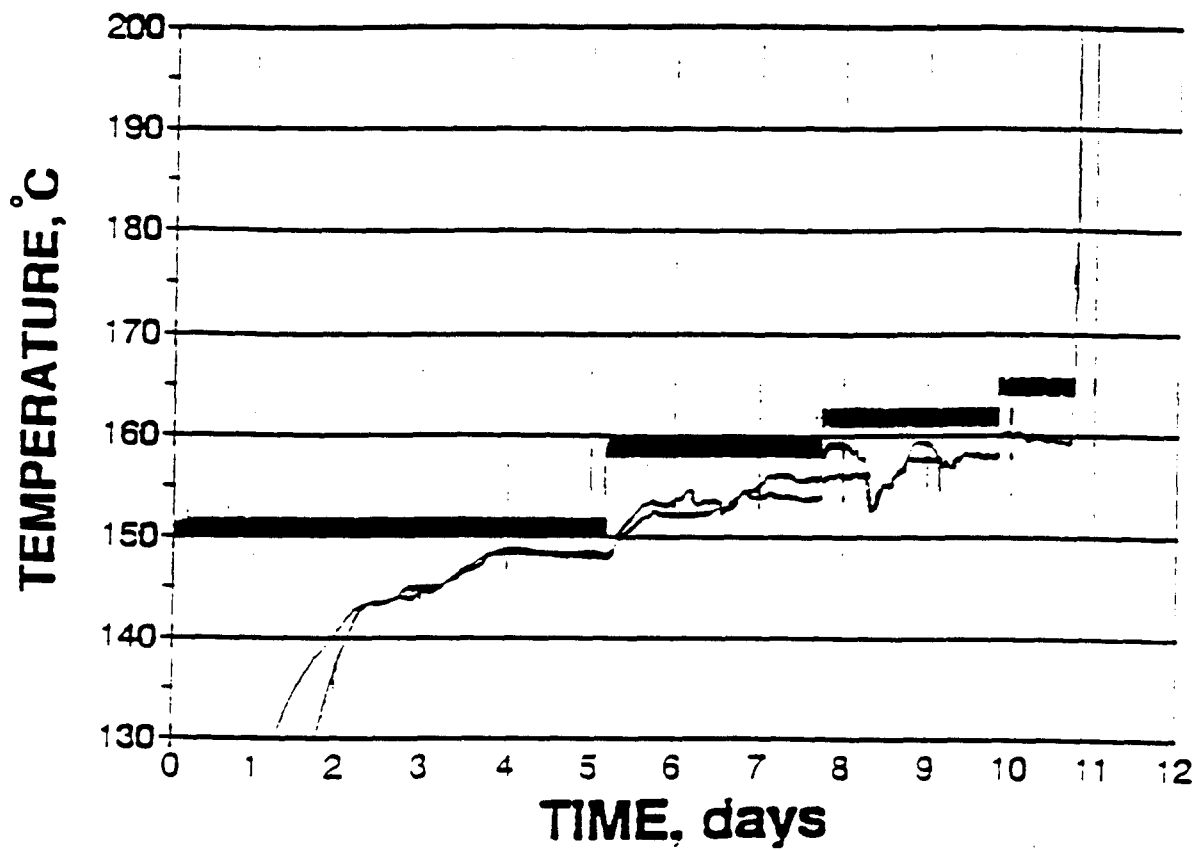


Figure 4-5. 32-liter cook-off data on expanded scale. The mid-radius thermocouple signal was lost at about 9.2 days.

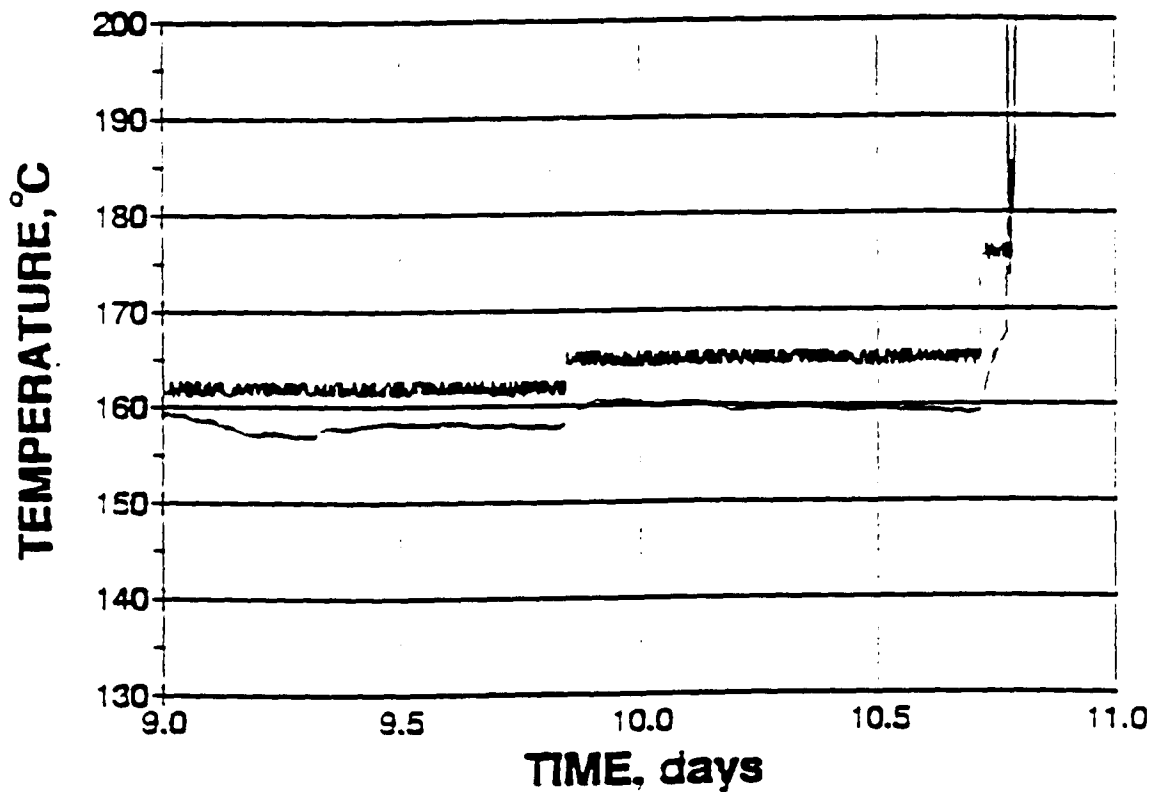


Figure 4-6. 32-liter cook-off data on expanded scale. The sample exhibited rapid self-heating soon after the temperature was increased at 10.75 days. The ANFO burned.

SECTION 5

DATA ANALYSIS

5.1 THERMAL CONDUCTIVITY OF ANFO.

An accurate value for the thermal conductivity of ANFO was needed to predict and analyze cook-off data and to make safety calculations for storing large quantities of ANFO and AN prills. An experimental thermal conductivity value was obtained by analyzing the temperature profiles during the first 150 minutes of one of the 1-liter cook-off tests²⁰. The ANFO did not begin to melt until after this time. The solid phase changes at 32, 84, and 125°C were evident in the temperature profiles (as is melting at later times). The endothermicity of these solid phase changes makes the thermal conductivity analysis uncertain, but we need an "engineering" value. By lumping the phase changes in with the heating processes, we obtained an effective thermal conductivity for practical use over this temperature range.

The 1-liter heat-up temperature profiles used for this analysis are shown in Figure 5-1. Also shown are temperature profiles calculated using Williams²¹ spreadsheet method and proposed values for the thermal conductivity. These calculations also required values for the density and specific heat of ANFO. The density was measured as $0.85 \pm 0.01 \text{ g/cm}^3$. A specific heat value from Urbanski²² was used of 1.5 J/(g K) , as measured for AN(III) at about 35-45°C. The value for the thermal conductivity of ANFO was varied until the calculated temperature profiles for the 1-liter test compared acceptably with the experimental data. Because of the phase changes, the fit was not as good as had been possible in previous work for emulsion and other materials. The final value determined for the thermal conductivity of ANFO was 0.11 W/(m K) , compared to that of high density AN of about 0.24 W/(m K) .²³

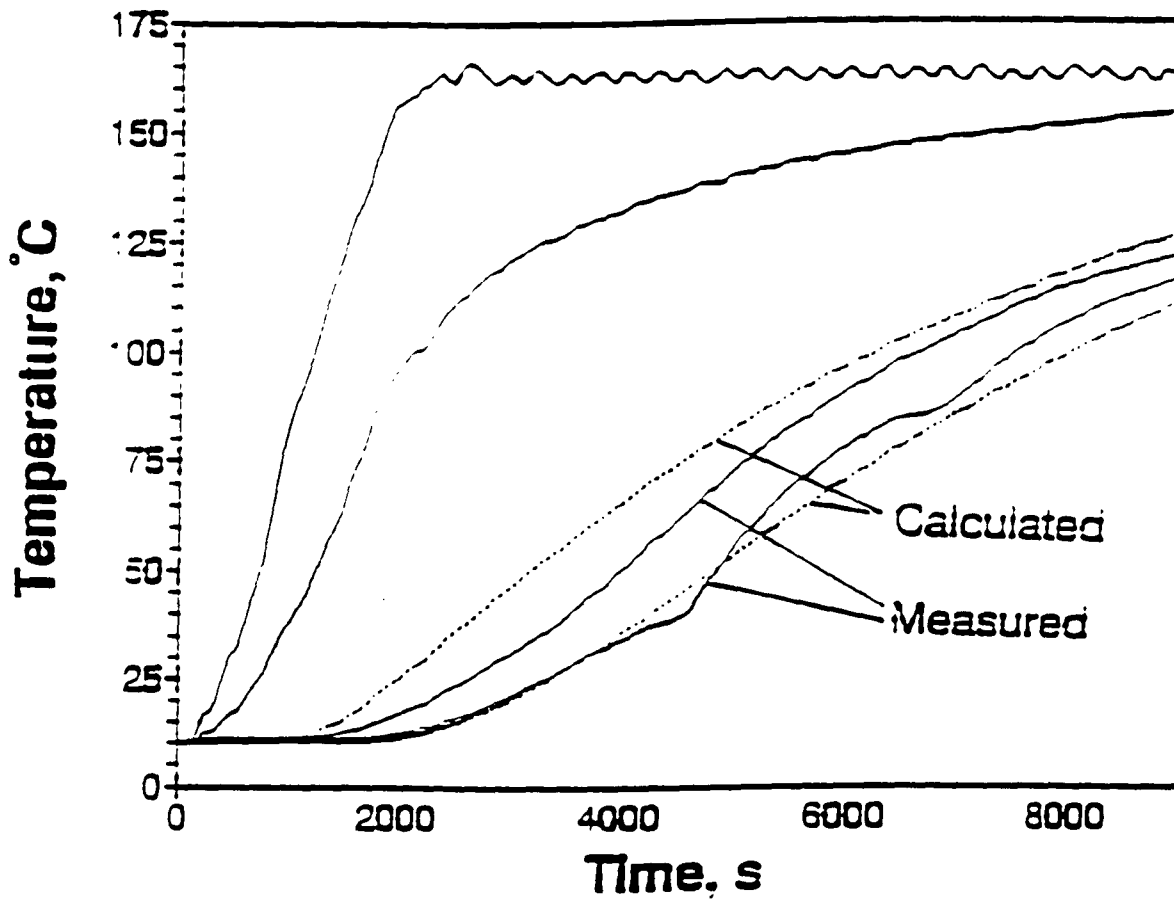


Figure 5-1. Thermal conductivity fit to 1-liter cook-off data on ANFO. The effective ANFO thermal conductivity was varied to fit the experimental data. Calculations were performed using 0.11 W/(m K) for the thermal conductivity, 1.5 J/g for the specific heat, and 0.85 g/cm³ for the density.

5.2 KINETIC ANALYSIS.

The three experimental critical temperatures from the Henkin, SSCB, and 32-liter cook-off tests were analyzed using the Frank-Kamenetskii formula to give reaction rate constants at each of the three temperatures. The following parameter values were used in the analysis:

- density of 1.65 g/cm³ (measured) for Henkin and 0.85 g/cm³ (measured) for SSCB and 32-liter
- thermal conductivity of 0.24 W/(m K) for Henkin and 0.11 W/(m K) for SSCB and 32-liter
- heat of reaction of 1260 J/g (300 cal/g)
- shape factors of 0.88 for Henkin, 2.5 for SSCB, and 2.7 for 32-liter

This analysis gave the following results:

Test	Weight	Radius	Critical Temperatur e	Shape Factor	Rate Constant
Henkin	0.04 g	0.035 cm	297°C	0.88	$1.2 \times 10^{-2} \text{s}^{-1}$
SSCB	25 g	0.79 cm	225°C	2.5	$2.5 \times 10^{-5} \text{s}^{-1}$
32-liter	22.7 kg	20.5 cm	168°C	2.7	$5.7 \times 10^{-8} \text{s}^{-1}$

The expression fitting these points (E_a in kcal/mol) is given below and shown in Figure 5-2.

$$\text{ANFO } k = 5.3 \times 10^{15} \exp(-46.04/RT) \text{ s}^{-1}$$

Also shown in Figure 5-2 are lines representing the ANMO data of Oxley, Kaushik, and Gilson and the FGAN data of Hainer over their respective temperature ranges. The agreement is excellent, even though the activation energies of the two earlier studies are lower than that of the current work. The current result for ANFO, the two AN/fuel results, and selected rate constants for AN are compared in Figure 5-3. The agreement between our Henkin point with the line from Oxley et al. is excellent, as is the agreement between our SSCB point and Hainer's FGAN data. Our ANFO data show a slower rate of decomposition than did Hainer's FGAN at about 165°C. Assuming that ANFO decomposes faster than AN by a factor of 2-5 times, the comparison with all of the AN work, except that of Robertson and Brower et al. (low T), is also excellent.

5.3 TOPAZ SIMULATIONS.

To test our ANFO kinetic and thermal parameters, we performed simulations of the SSCB and 32-liter cook-off tests using a PC version of the thermal code TOPAZ. TOPAZ-2D is a

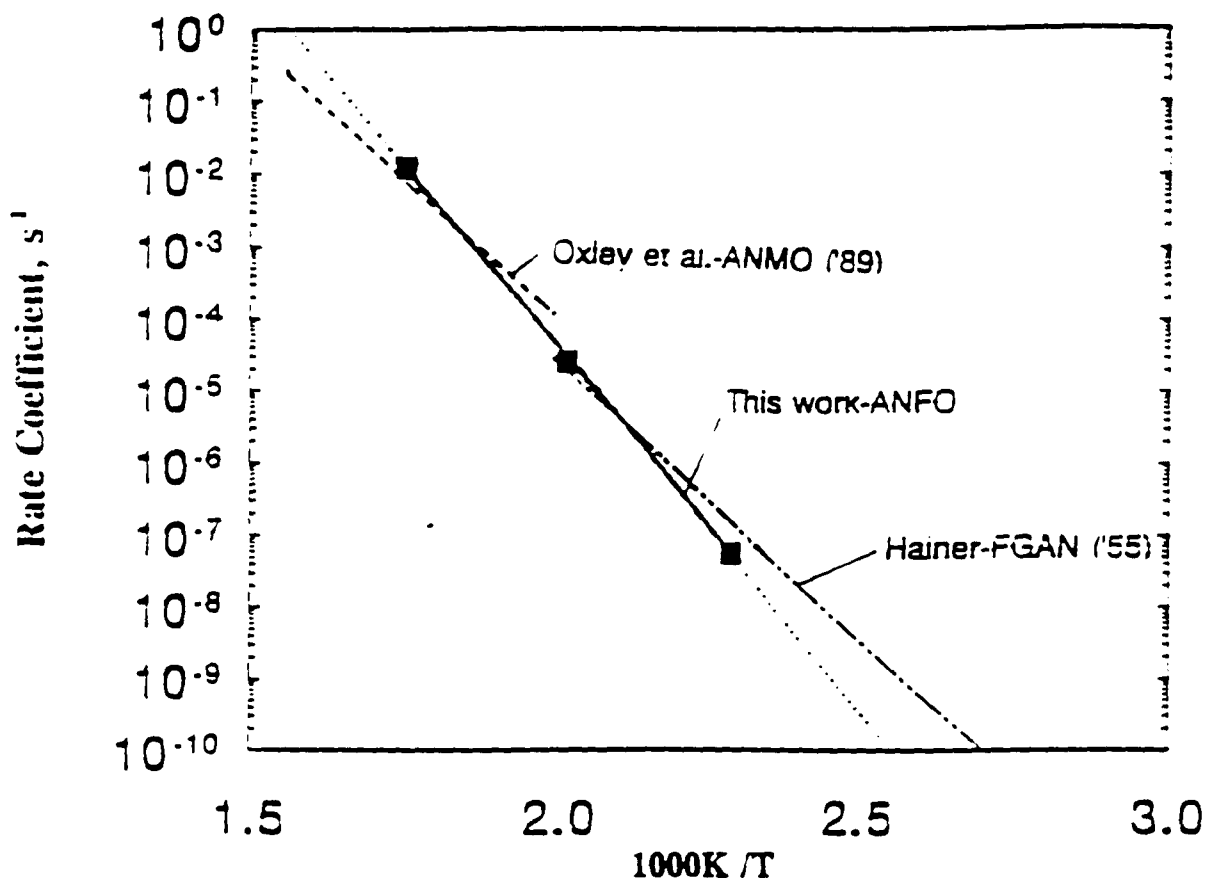


Figure 5-2. Arrhenius graph of ANFO decomposition data. The filled points are the experimental data from this work. The expressions of Oxley et al. and of Hainer are shown for comparison.

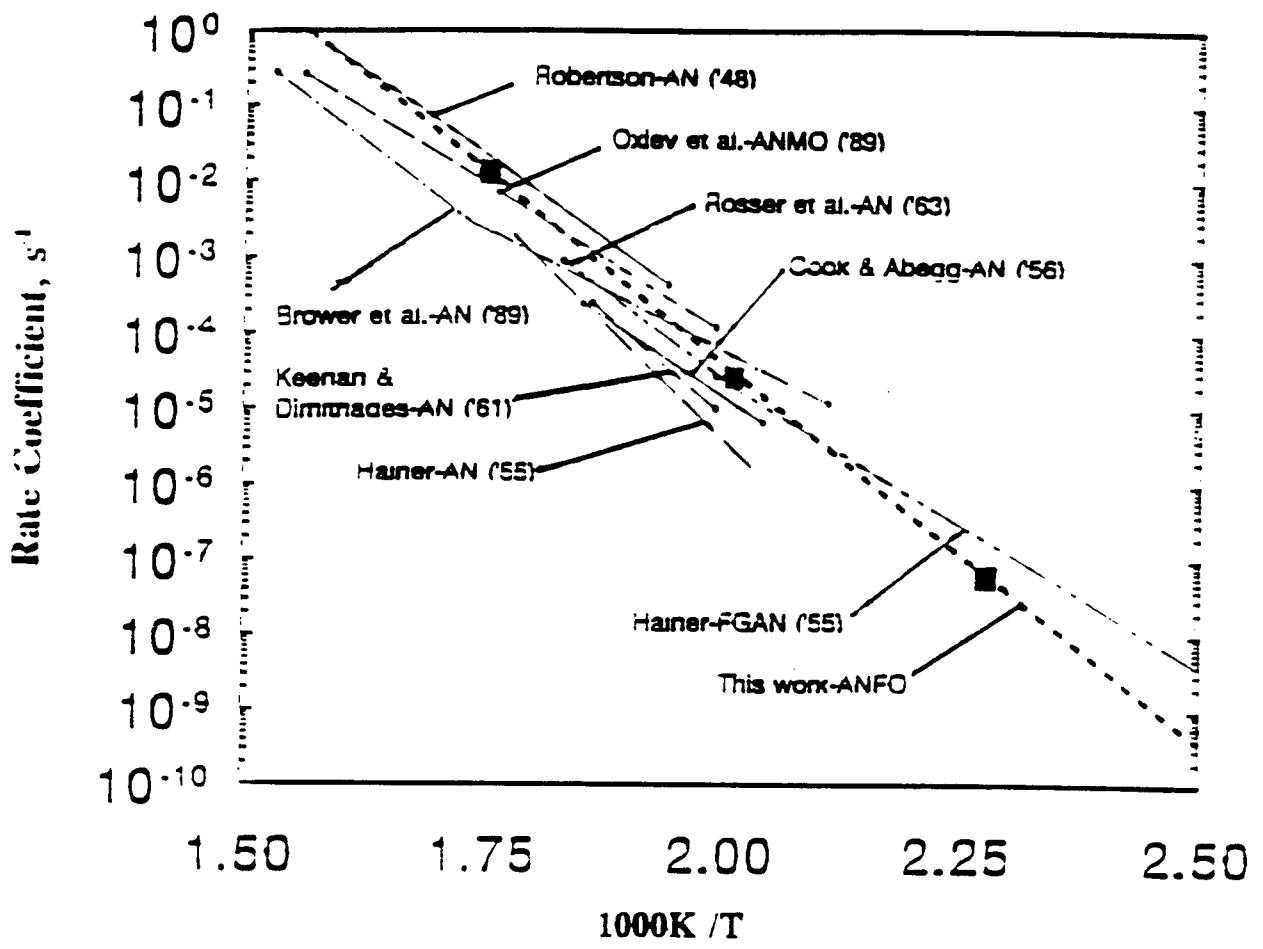


Figure 5-3. Comparison of current and literature data on ANFO and AN.

two-dimensional implicit finite element computer code for simulating chemical decomposition, heat transfer, and other problems. The code, which was originally written at LLNL²⁴, can be used to solve steady-state and transient temperature fields for two-dimensional planar or axisymmetric geometries. Constant, isotropic properties for the explosive were used in this work. Chemical kinetics were modeled as a single, first-order reaction. A Turbo Pascal version²⁵ of TOPAZ-2D (hereafter referred to as TOPAZ) was used in this work and run on a 33 MHz 486 PC.

The model of the SSCB apparatus was developed using 14 points (nodes) defining 6 volume elements. The aluminum walls of the vessel, as well as the explosive, were included in the model. The outer wall temperature boundary condition included the finite time to reach the test temperature.

The TOPAZ model of the 32-liter apparatus included 77 nodes defining 60 volume elements. The glass walls of the vessel, as well as the air space between the ANFO and the heated vessel lid, were included in the model. The temperature boundary conditions were applied to the top, bottom, and sides of the vessel. The specific heating history of test #2 was used in the calculations.

The results of the two series of TOPAZ calculations are summarized below.

Test	Temp.	Rate Constant	Time to Runaway	
			Experiment	Calc.
SSCB	230	Standard	40 min	35 min
"	"	Std *0.50	"	No runaway
"	"	Std *0.75	"	45 min
"	220	Standard	No runaway	No runaway
32-liter	Test Profile	Standard	10.77 days	12.12 days
"	"	Std *0.50	"	14.47 days
"	"	Std * 2	"	11.16 days
"	"	Std * 5	"	7.07 days

In simulating the SSCB test at 230°C, we initially used the ANFO decomposition rate constant determined in this work (denoted as "standard"). The TOPAZ calculation showed thermal runaway slightly faster than observed (35 minutes vs. 40 minutes observed). Although this is excellent agreement, a few additional runs were made to determine the sensitivity of the calculations to changes in the rate constant. When the rate constant was divided by 2, no runaway was computed. When it was reduced by 25 percent, runaway was calculated at 45 minutes. Thus the rate constant expression is probably accurate within about

10 percent at 230°C.

At 220°C, where no SSCB runaway was experimentally observed, the standard rate constant expression gave no computed runaway.

In the TOPAZ simulations of the 32-liter cook-off tests, the standard rate constant gave runaway slightly slower than was observed. Multiplying and dividing the rate constant by 2 and then multiplying by 5 gave results that indicate that the rate constant expression may be slightly low, by about a factor of 2, in the temperature region of 150-165°C. This uncertainty is about the same magnitude as the square points which represent the data in Figure 5-2.

Overall, agreement between calculated and experimental time to runaway is excellent for the SSCB tests and good for the 32-liter test. The temperature profiles from the 32-liter test indicate that the experiment is more complex than the simple model.

5.4 APPLICATIONS TO LARGE CHARGES.

With reason to think that extrapolation of the ANFO thermal stability model calculations on large storage quantities should be reasonably valid, we performed some calculations on field applications.

5.5 F-K CALCULATIONS.

The variation of critical temperatures for ANFO cylinders and spheres with increasing radius was calculated using the simple F-K formula and the input parameters discussed above. Figure 5-4 shows these minimum runaway temperatures for cylinders. The critical temperatures lie in the range from 160 to 140°C for cylinders with radius from about 25 to 150 cm. As a point of reference, a 55-gallon drum has a radius of about 28 cm and would weigh about 175 kg (385 pounds) when filled with ANFO. The critical temperature for such a drum would be 158°C. A 1-ton cylinder with diameter equal to length would have a diameter of 55 cm and a critical temperature of 147°C.

Critical temperatures similarly calculated using the F-K formula for spherical quantities of ANFO are shown vs. charge weight on a logarithmic scale in Figure 5-5. The linear relationship shown in this figure indicates that the critical temperatures decrease by about 10°C for every ten-fold increase in the mass of ANFO. Note that these calculations were performed for spherical configurations of ANFO, but that the results are not very sensitive to the shape of the mass, as long as it is relatively compact. The critical temperature for 2,000 tons is seen in Figure 5-5 to be about 110°C (230°F).

Specific calculations were performed for hemispheres of 2,400 and 4,800 tons of ANFO. These charges would have radii of 1070 and 1347 cm, respectively, at a density of 0.85 g/cm³. F-K calculations were performed using these radii, the model parameters given above,

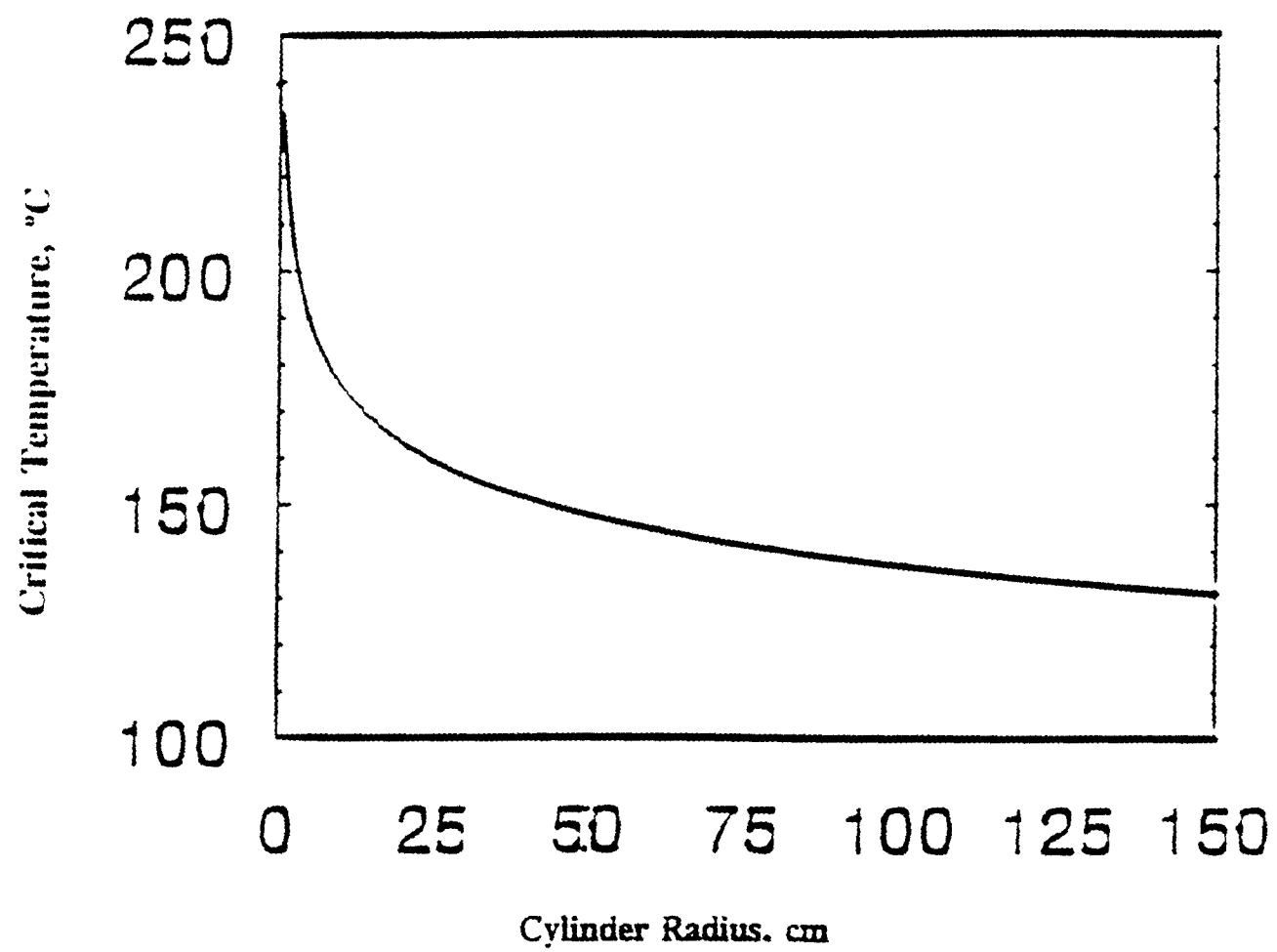


Figure 5-4. Calculated critical temperatures for ANFO cylinders. Predictions made using the F-K formula and input parameters discussed in the text.

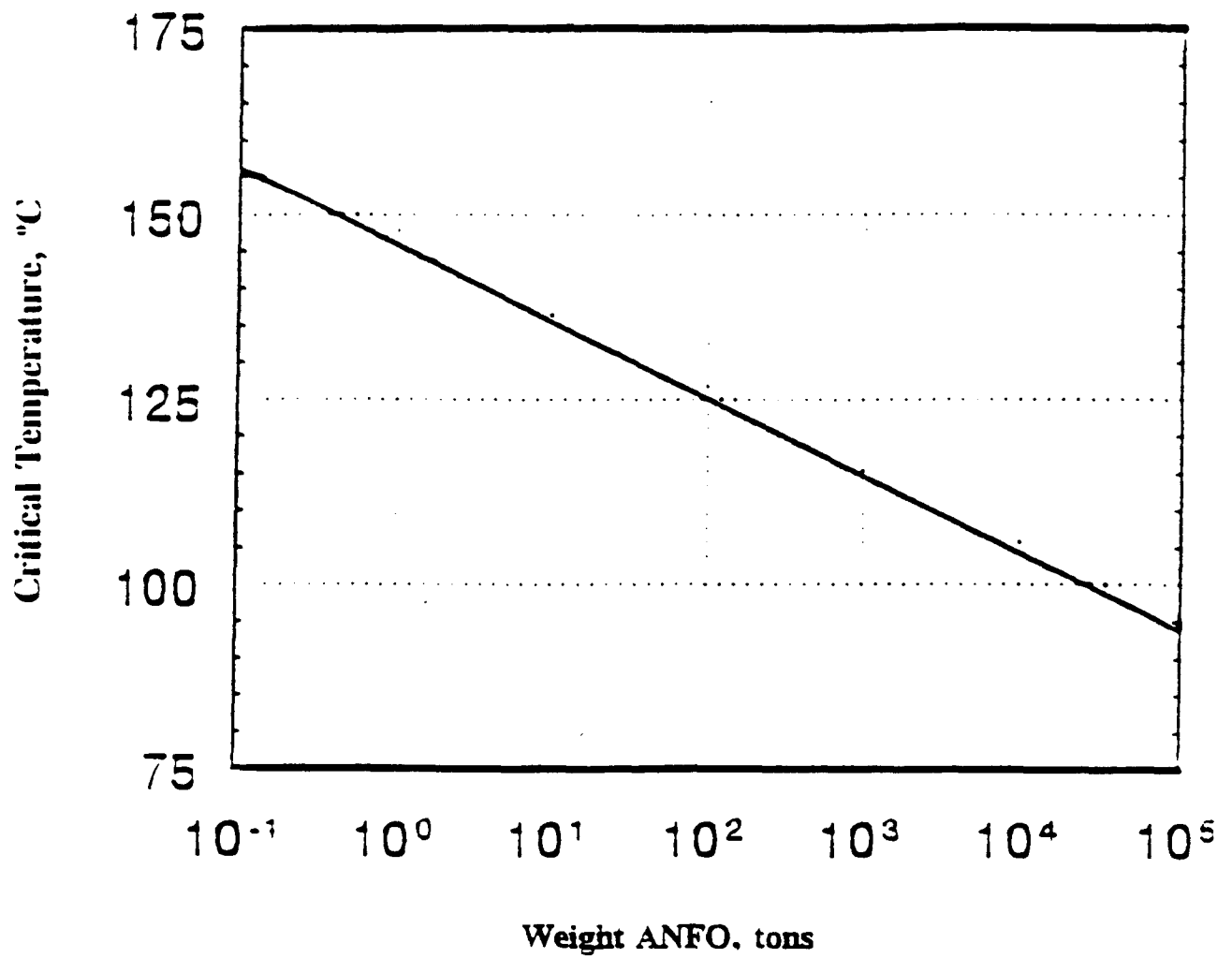


Figure 5-5. Calculated critical temperatures for large ANFO spheres. Predictions made using the F-K formula and input parameters discussed in the text.

and a shape factor of 3.33 (sphere), ignoring that the charges were only half spheres. This assumes that the interface between the ANFO and the ground is approximately adiabatic (no heat loss), which is probably a good assumption. Critical temperatures are given below for the standard rate constant, and for the rate constant multiplied and divided by a factor of two. Since the uncertainty in the rate constant is thought to be less than this factor, a conservative range of critical temperatures were calculated to include this and other uncertainties.

ANFO Charge Size	Critical Temperature		
	Standard	Std. x 2	Std. / 2
2,400 tons	107°C	103°C	112°C
4,800 tons	104°C	100°C	109°C

Thus the final F-K results are $107 \pm 4^\circ\text{C}$ and $104 \pm 4^\circ\text{C}$ for the 2,400 and 4,800-ton charge sizes.

5.6 TOPAZ CALCULATIONS.

A TOPAZ model of a 2,400-ton hemisphere of ANFO (radius = 1067 cm) was created using 42 nodal points defining 31 volume elements. Because of the large size of the charge, the thermal effects of the container were ignored. (Fiberglass is a good heat conductor compared with ANFO.)

The first calculations were made using a constant elevated temperature boundary condition at the outside surface of the charge. Runs were made with this temperature set to 110, 125, and 140°C , with the initial ANFO temperature at 35°C . The calculations were run to simulate a 30-day period under these conditions. No thermal runaway occurred in these calculations; in fact, the ANFO is such a good thermal insulator that the temperature increase was limited to the material near the surface of the container. Another simulation was run with the surface temperature at 165°C , well above the critical temperature, and the initial ANFO temperature at 80°C . Although the temperature of the material near the surface exceeded 100°C , no significant heat generation or runaway was seen.

We concluded that heating in this manner (i.e., by conduction from the outside surface of the hemisphere) cannot create a runaway situation in any credible scenario.

5.7 ANFO FIRE HAZARDS.

Another possible hazard situation would be a fire in part of the ANFO charge which might heat the adjacent ANFO to thermal runaway or accelerate to a deflagration to detonation (DDT) transition. Wang²⁶ previously performed some pressurized burning tests on ANFO and ANFO with 10 wt% aluminum (Alcoa 1620A). The material was ignited using Reynolds Industries Systems, Inc. SQ-80 thermite-filled exploding bridgewire ignitors located

approximately 2.5 cm above the samples. These tests were considered preliminary, but additional tests were not performed.

	"No-Go" Pressure (MPa)	"Go" Pressure (MPa)
ANFO	4.1	4.8
ANFO + Al	1.73	2.76

Note, however, that in a later test on ANFO at 5.5 MPa, the combustion failed to propagate through the complete sample.

A few linear burn rate (LBR) tests were performed on ANFO + 10 wt% aluminum using squib ignitors, 2.5 cm diameter glass tubes, and fuse wires for measuring the burning front arrival at selected locations along the tube. These data should also be considered preliminary. Tests were performed at two pressures.

Initial Pressure (MPa)	Average Pressure (MPa)	LBR (cm/s)
5.52	7.41	1.626
4.14	5.17	0.798

These data show two main points. First, for small samples, ANFO at room temperature and atmospheric pressure does not readily burn. This may not be true if scaled to large quantities of material where heat losses would be reduced. In our 32-liter cook-off tests, we burned most of the ANFO, but the material was initially quite hot, just below the melting temperature. Once ignited, melting of ANFO at approximately 169°C also may help since the molten material may flow away from the fire area. All of the ANFO was not consumed in the fires that resulted from burning the 32-liter test charges.

The second point from Wang's data is that, at least for the aluminized ANFO that was tested, the burn rate is rather high at 1-2 cm/s under the high pressure conditions tested. However, in ambient fires, these pressures would be difficult to achieve.

SECTION 6

CONCLUSIONS

Overall, the work reported here showed ANFO to be a highly thermally stable energetic material, suitable for use in large conventional explosive charges. The data measured in this work allow predictions of minimum thermal runaway conditions for ANFO charges of various sizes and for various initial conditions. If the initial ANFO temperature loaded into a container such as a hemisphere of 2,400 tons (10 meters radius, 70 feet in diameter) is near ambient, our model indicates that no credible external heating is likely to bring the material to a runaway condition. The main remaining hazards are from a large fire at the surface or inside the ANFO, or in some other nearby fuel, or from accidental detonation of some other explosive, such as a high explosive booster charge, near the ANFO.

Specifically, the following tasks were accomplished in this program:

- The effective thermal conductivity of solid ANFO was measured as 0.11 W/(m K) using a specific heat value of 1.5 J/(g K).
- Isothermal cook-off tests were performed on samples ranging from 0.04 g to approximately 25 kg.
- These cook-off data have been used to give the thermal stability of ANFO from 168 to 297°C—a range covering over five decades in reaction rates. The resulting Arrhenius rate constant expression was:

$$k = 5.3 \times 10^{15} \exp(-46.04/RT) \text{ s}^{-1} .$$

- These data compare favorably with previous studies on AN/fuel mixtures.
- Minimum thermal runaway temperatures were calculated for large storage quantities of ANFO.

SECTION 7

REFERENCES

1. Zeldovitch, Ya.B.; Barenblatt, G.I.; Librovich, V.B.; and Makhviladze, G.M. "The Time-Independent Theory of Thermal Explosions." In *The Mathematical Theory of Combustion and Explosions*. Plenum Press: New York, 1985, pp. 143-185, (UNCLASSIFIED).
2. Frank-Kamenetskii, D.A. *Diffusion and Heat Exchange in Chemical Kinetics*. Princeton University Press, 1955, (UNCLASSIFIED).
3. Gray, P. and Lee, P.R. *Oxid. Combust. Rev.*, **1967**, *2*, 1, (UNCLASSIFIED).
4. Zinn, J. and Mader, C. "Thermal Initiation of Explosives." *J. Appl. Phys.*, **1960**, *31*, 323, (UNCLASSIFIED).
5. Zinn, J. and Rogers, R. "Thermal Initiation of Explosives." *J. Phys. Chem.*, **1962**, *66*, 2646, (UNCLASSIFIED).
6. Senenov, N.N. *Chemical Kinetics and Chain Reactions*. Oxford Univ. Press: London, 1935, (UNCLASSIFIED).
7. Rogers, R.N.; Guiana, J.L.; and Loverro, N.P., Jr. *J. Energetic Materials*, **1984**, *2*, 293, (UNCLASSIFIED).
8. Cook, M.A. *The Science of Industrial Explosives*, (IRECO CHEMICALS, 1974), (UNCLASSIFIED).
9. Hainer, R.M. "The Application of Kinetics to the Hazardous Behavior of Ammonium Nitrate." Fifth Symposium (International) on Combustion (Reinhold Publishing Co., New York, 1955, p. 224.), (UNCLASSIFIED).
10. Oxley, J.C; Kaushik, S.; and Gilson, N. *Thermochemica Acta*, **1989**, *153*, 269, (UNCLASSIFIED).
11. King, A. and Bauer, A. "A Critical Review of the Thermal Decomposition Mechanisms of Ammonium Nitrate." Report to the Canadian Fertilizer Institute and Contributing Bodies, Queen's University, Kingston Ontario, 1982, (UNCLASSIFIED).
12. Robertson, J. *Chem. Soc. Ind.*, **1948**, *67*, 221, (UNCLASSIFIED).

13. Cook, M.A. and Abegg, M.T. *Ind. Engr. Chem.* **1956**, *48*, 1090, (UNCLASSIFIED).
14. Keenan, A.G. and Dimitriadis, B. *Trans. Faraday Soc.*, **1961**, *57*, 1019, (UNCLASSIFIED).
15. Rosser, W.A.; Inami, S.H.; and Wise, H. *J. Chem. Phys.*, **1963**, *67*, 1753, (UNCLASSIFIED).
16. Brower, K.R.; Oxley, J.C.; and Tewari, M. "Evidence for Homolytic Decomposition of Ammonium Nitrate at High Temperatures." *J. Phys. Chem.*, **1989**, *93*, 4029, (UNCLASSIFIED).
17. Henkin, H. and McGill, R. "Rates of Explosive Decomposition of Explosives." *Ind. Engr. Chem.*, **1952**, *44*, 1391, (UNCLASSIFIED).
18. Rogers, R.N. *Thermochemica Acta*, **1975**, *11*, 131-139, (UNCLASSIFIED).
19. Pakulak, J.M., Jr. and Cragin, S. "Calibration of a Super Small-Scale Cook-off Bomb (SSCB) for predicting Severity of the Cook-off Reaction." Naval Weapons Center, China Lake, CA, NWC TP 6414, July 1983, (UNCLASSIFIED).
20. Olson, RCEM Report A-01-92, April 1992, (UNCLASSIFIED).
21. Williams, P.E. In RCEM Report No. A-02-93, "Thermal Conductivity of Energetic Materials" submitted to members of the Research Center for Energetic Materials, New Mexico Tech, Socorro, NM, 1993, (UNCLASSIFIED).
22. Urbanski, T. *Chemistry and Technology of Explosives*. Pergamon Press: New York, 1965, (UNCLASSIFIED).
23. Block-Bolten, A.; Grant, M.; and Olson, D. RCEM Report No. A-02-93, "Thermal Conductivity of Energetic Materials" submitted to members of the Research Center for Energetic Materials, New Mexico Tech, Socorro, NM, 1993, (UNCLASSIFIED).
24. Shapiro, A. TOPAZ 2D-A *Two-dimensional Finite Element Code for Heat Transfer Analysis, Electrostatic, and Magneto Static Problems*, Lawrence Livermore National Laboratory Report UCID-20824, July 1986, (UNCLASSIFIED).
25. Ostmark, H. and Roman, N. TOPAZ for PC, personal communication, (UNCLASSIFIED).
26. Wang, J. "Ignition and Combustion Characteristics of Emulsion Explosives Under Pressure. M.S. Thesis, October 1991, (UNCLASSIFIED).

Appendix

Henkin Data for ANFO

Sample	Weight [mg]	Thick mm	Temperature [C] [K]		Time [s]	1000/T [1/K]	log(time)	Notes
# 2	39.2	0.69	272	545	1200	1.8349	3.0792	No Go
# 3	41.1	0.76	286	559	1200	1.7889	3.0792	No Go
# 4	40.1	0.71	296	569	1200	1.7575	3.0792	No Go
#25	39.2	0.70	297	570	1200	1.7544	3.0792	No Go
#26	40.3	0.70	297	570	55.00	1.7544	1.7404	Go
#12	39.6	0.70	298	571	25.91	1.7513	1.4135	Go
#15	39.3	0.70	298	571	600	1.7513	2.7782	No Go
#16	40.7	0.73	298	571	1200	1.7513	3.0792	No Go
#24	41.1	0.69	298	571	1080	1.7513	3.0334	No Go
#27	40.8	0.70	298	571	29.41	1.7513	1.4685	Go
#19	39.6	0.73	299	572	1200	1.7483	3.0792	No Go
#23	40.6	0.71	299	572	28.87	1.7483	1.4604	Go
#13	40.2	0.69	300	573	23.09	1.7452	1.3634	Go
#17	39.9	0.71	300	573	1200	1.7452	3.0792	No Go
#14	40.3	0.70	302	575	23.16	1.7391	1.3647	Go
#18	40.0	0.72	302	575	24.36	1.7391	1.3867	Go
# 8	40.3	0.72	304	577	22.88	1.7331	1.3595	Go
# 7	40.7	0.73	306	579	16.84	1.7271	1.2263	Go
# 6	40.6	0.70	308	581	17.05	1.7212	1.2317	Go
# 5	40.1	0.69	310	583	15.37	1.7153	1.1867	Go
#21	40.6	0.71	312	585	17.36	1.7094	1.2395	Go
#22	39.9	0.69	314	587	11.76	1.7036	1.0704	Go
# 9	40.3	0.68	315	588	480	1.7007	2.6812	No Go
#11	41.0	0.70	315	588	10.34	1.7007	1.0145	Go
#20	40.5	0.73	317	590	8.70	1.6949	0.9395	Go
#10	40.8	0.72	320	593	10.63	1.6863	1.0265	Go

DISTRIBUTION LIST

POR 7547

DEPARTMENT OF DEFENSE

ADVANCED RESEARCH PROJECT AGENCY
ATTN: DIR AEROSPACE & STRATEGIC TECH OFC

ASSISTANT TO THE SECRETARY OF DEFENSE
ATTN: EXECUTIVE ASSISTANT

DEFENSE INTELLIGENCE AGENCY
ATTN: DGI4

DEFENSE NUCLEAR AGENCY
ATTN: DDIR G ULLRICH
ATTN: DFTD
2 CY ATTN: IMTS
ATTN: OTA DR P CASTLEBERRY
ATTN: OTA R ROHR
ATTN: SPSD
ATTN: SPSD M GILTRUD
ATTN: SPSD MAJ ALTY
ATTN: SPSD MAJ M ABERNATHY
ATTN: SPSP
ATTN: SPSP T FREDERICKSON
ATTN: SPWE
ATTN: SPWE K PETERSEN
ATTN: SPWE LEON A WITTER
ATTN: TASS DR C GALLOWAY
ATTN: TDTR
ATTN: TDTR G FRITZ
ATTN: TDTR M FLOHR

DEFENSE TECHNICAL INFORMATION CENTER
2 CY ATTN: DTIC/OC

FIELD COMMAND DEFENSE NUCLEAR AGENCY
ATTN: FCT
ATTN: FCTC R SMITH
ATTN: FCTI G S LU
ATTN: FCTIP K SHAH
ATTN: FCTM
ATTN: FCTO
ATTN: FCTO DR LEECH
ATTN: FCTOE
ATTN: FCTOH
10 CY ATTN: FCTT-T E RINEHART
ATTN: FCTT DR BALADI
ATTN: FCTT J HUGHES
ATTN: FCTTD LT COL ROWE
ATTN: FCTTS G GOODFELLOW
ATTN: FCTTS LTCOL LEONARD
ATTN: FCTTS R MCCRORY
ATTN: FCTTS E MARTINEZ

UNDER SECRETARY OF DEFENSE (ACQ)
ATTN: DENNIS J GRANATO

DEPARTMENT OF THE ARMY

ARMY RESEARCH LABORATORIES
ATTN: TECH LIB
ATTN: DELHD-TA-L

DEP CH OF STAFF FOR OPS & PLANS
ATTN: DAMO-SWN

PED MISSILE DEFENSE SFAE-MD-TSD
ATTN: CSSD-SA-EV
ATTN: CSSD-SL

U S ARMY AVIATION CTR & FT RUCKER
ATTN: ATZQ-CDC-C TORRENCE

U S ARMY AVIATION SYSTEMS CMD
ATTN: AMCPEO-LHX-TV D DEIBLER

U S ARMY BALLISTIC RESEARCH LAB
ATTN: AMSRL-WT-NC J SULLIVAN
2 CY ATTN: SLCBR-SS-T
ATTN: SLCBR-TB-B J POLK
ATTN: SLCBR-TBD P MULLER

U S ARMY COMM R&D COMMAND DEFENSE CMD
ATTN: CSSD-SA-E
ATTN: CSSD-SD-A

U S ARMY CORPS OF ENGINEERS
ATTN: CERD-L
ATTN: DAEN-RDL

U S ARMY ENGINEER DIV HUNTSVILLE
ATTN: HNDED-SY

U S ARMY ENGR WATERWAYS EXPER STATION
ATTN: C WELCH CEWES-SE-R
ATTN: CEWES J K INGRAM
ATTN: CEWES-SD
ATTN: CEWES-SS-R DR BALSARA
ATTN: J ZELASKO CEWES-SD-R
ATTN: RESEARCH LIBRARY
ATTN: TECHNICAL LIBRARY

U S ARMY FOREIGN SCIENCE & TECH CTR
ATTN: DRXST-SD
ATTN: IAFSTC-RMT

U S ARMY NUCLEAR & CHEMICAL AGENCY
ATTN: LIBRARY
ATTN: MONA-NU DR D BASH

U S ARMY RESEARCH DEV & ENGRG CTR
ATTN: STRNC-YSD G CALDARELLA

U S ARMY WAR COLLEGE
ATTN: LIBRARY

USA CML & BIOLOGICAL DEFENSE AGENCY
ATTN: AMSCB-BDL J CANNALIATO

DEPARTMENT OF THE NAVY

DAVID TAYLOR RESEARCH CENTER
ATTN: M CRITCHFIELD CODE 1730.2

DEPARTMENT OF THE NAVY
ATTN: CODE R44 R FERGUSON
ATTN: CODE R44 P COLLINS
ATTN: TECH LIB E232

NAVAIRWARCENWPNDIV
ATTN: CODE 343

POR 7547 (DL CONTINUED)

NAVAL POSTGRADUATE SCHOOL
ATTN: CODE 52 LIBRARY

NAVAL RESEARCH LABORATORY
ATTN: CODE 2600 TECHNICAL LIBRARY
ATTN: CODE 4040 D BOOK
ATTN: CODE 4400 J BORIS
ATTN: CODE 5227 RESEARCH REPORT

NAVAL SURFACE WARFARE CENTER
ATTN: CODE H-23 R PERSH

NAVAL UNDERWATER SYS CENTER
ATTN: TECH LIB

NAWCWPNSDIV DETACHMENT
ATTN: CLASSIFIED LIBRARY

NFESC
ATTN: CODE L-64 J MATTHEWS
ATTN: CODE L64 LORY

OFFICE OF CHIEF NAVAL OPERATIONS
ATTN: OP 03EG

OFFICE OF NAVAL RESEARCH
ATTN: CODE 1132SM

DEPARTMENT OF THE AIR FORCE

AIR COMBAT COMMAND
ATTN: LT COL R EASTERLIN

AIR UNIVERSITY LIBRARY
ATTN: AUL-LSE

HEADQUARTERS USAF/IN
ATTN: IN

PHILLIPS LABORATORY
2 CY ATTN: OL/NS

US AIR FORCE/FSTC
ATTN: CAPT WHITWORTH

WRIGHT RESEARCH & DEVELOPMENT CENTER
ATTN:ATTN: D RICHMOND

DEPARTMENT OF ENERGY

DPEARTMENT OF ENERGY
ATTN: DR C V CHESTER

LAWRENCE LIVERMORE NATIONAL LAB
ATTN: C E ROSENKILDE
ATTN: J BELL
ATTN: R PERRETT
ATTN: TECH LIBRARY

LAWRENCE LIVERMORE NATIONAL LABORATORY
ATTN: ALLEN KUHL

LOS ALAMOS NATIONAL LABORATORY
ATTN: REPORT LIBRARY
ATTN: REPORT LIBRARY

SANDIA NATIONAL LABORATORIES
ATTN: A CHABAI DEPT-9311
ATTN: DIV 9114 A SEHMER
ATTN: DIV 9311 L R HILL
ATTN: TECH LIB 3141

U S DEPARTMENT OF ENERGY
OFFICE OF MILITARY APPLICATIONS
ATTN: OMA/DP-252 MAJ D WADE

OTHER GOVERNMENT

CENTRAL INTELLIGENCE AGENCY
ATTN: OSWR/NED 5S09 NHB

DEPARTMENT OF DEFENSE CONTRACTORS

AEROSPACE CORP
ATTN: D LYNCH
ATTN: H MIRELS
ATTN: LIBRARY ACQUISITION

APPLIED & THEORETICAL MECHANICS. INC
ATTN: J M CHAMPNEY

APPLIED RESEARCH ASSOCIATES
ATTN: R FLORY

APPLIED RESEARCH ASSOCIATES. INC
ATTN: J KEEFER
ATTN: N ETHRIDGE

APPLIED RESEARCH ASSOCIATES. INC
ATTN: C J HIGGINS
ATTN: D COLE
ATTN: J L BRATTON
3 CY ATTN: K BELL
ATTN: N BAUM

APPLIED RESEARCH ASSOCIATES. INC
ATTN: R FRANK

APPLIED RESEARCH ASSOCIATES. INC
ATTN: J L DRAKE

APPLIED RESEARCH INC
ATTN: J BOSCHMA

ARES CORP
ATTN: A DEVERILL

ARES CORP
ATTN: J WEICHEL

AUTOMETRIC. INC
ATTN: P RICHARD

BDM FEDERAL INC
ATTN: E DORCHAK
ATTN: J STOCKTON

BDM FEDERAL INC
ATTN: LIBRARY

CALSPAN CORP
ATTN: LIBRARY

CARPENTER RESEARCH CORP ATTN: H J CARPENTER	LOGICON R & D ASSOCIATES ATTN: B KILLIAN
DENVER RESEARCH INSTITUTE ATTN: JOHN WISOTSKI ATTN: L BROWN	LOGICON R & D ASSOCIATES ATTN: G GANONG 3 CY ATTN: J RENICK ATTN: J WALTON
E-SYSTEMS, INC ATTN: TECH INFO CTR	LOGICON R & D ASSOCIATES ATTN: E FURBEE ATTN: J WEBSTER
EG&G MANAGEMENT SYSTEMS, INC ATTN: J YELVERTON	LORAL VOUTHG SYSTEMS CORP 2 CY ATTN: LIBRARY EM-08
FLUID PHYSICS IND ATTN: R TRACI	MAXWELL LABORATORIES INC ATTN: C PETERSEN ATTN: G SCHNEYER ATTN: J BARTHEL ATTN: K D PYATT JR ATTN: LIBRARY ATTN: P COLEMAN ATTN: T PIERCE
GEO CENTERS, INC ATTN: B NELSON	MCDONNELL DOUGLAS CORPORATION ATTN: R HALPRIN
HORIZONS TECHNOLOGY, INC ATTN: E TAGGART	MISSION RESEARCH CORP ATTN: TECH LIBRARY
IIT RESEARCH INSTITUTE ATTN: DOCUMENTS LIBRARY ATTN: M JOHNSON	MOLZEN CORBIN & ASSOCIATES, P.A. ATTN: TECHNICAL LIBRARY
INFORMATION SCIENCE, INC ATTN: W DUDZIAK	NICHOLS RESEARCH CORPORATION ATTN: R BYRN
INSTITUTE FOR DEFENSE ANALYSES ATTN: CLASSIFIED LIBRARY	PACIFIC-SIERRA RESEARCH CORP ATTN: H BRODE ATTN: R LUTOMIRSKI 36 CY ATTN: S FUGIMURA
JAYCOR ATTN: CYRUS P KNOWLES	PACIFIC-SIERRA RESEARCH CORP ATTN: M ALLERDING
KAMAN SCIENCES CORP ATTN: D CAYNE ATTN: LIBRARY ATTN: R RUETENIK	PHYSICAL RESEARCH INC ATTN: D MODARRESS
KAMAN SCIENCES CORP ATTN: JOHN KEITH	PHYSITRON INC ATTN: M PRICE
KAMAN SCIENCES CORP ATTN: D MOFFETT 2 CY ATTN: DASIAC	S-CUBED ATTN: C NEEDHAM ATTN: K SCHNEIDER
KAMAN SCIENCES CORPORATION 2 CY ATTN: DASIAC ATTN: K GOULD	SCIENCE APPLICATIONS INTL CORP ATTN: C HSIAO ATTN: F Y SU ATTN: G EGGUM ATTN: G T PHILLIPS ATTN: H WILSON ATTN: R ALLEN ATTN: TECH LIBRARY ATTN: TECHNICAL REPORT SYSTEM
KARAGOZIAN AND CASE ATTN: J KARAGOZIAN	SCIENCE APPLICATIONS INTL CORP ATTN: DIV 411 R WESTERFELDT
KTECH CORP ATTN: D JOHNSON	
LOCKHEED MISSILES & SPACE CO, INC ATTN: TECH INFO CTR	
LOGICON R & D ASSOCIATES ATTN: C K B LEE ATTN: D SIMONS ATTN: DOUGLAS C YOON ATTN: LIBRARY ATTN: R GILBERT	

POR 7547 (DL CONTINUED)

SCIENCE APPLICATIONS INTL CORP ATTN: J GUEST	TITAN CORPORATION (THE) ATTN: D HATFIELD
SCIENCE APPLICATIONS INTL CORP 2 CY ATTN: H SINGER	2 CY ATTN: F SAUER
ATTN: J COCKAYNE	ATTN: LIBRARY
ATTN: W LAYSON	TRW INC
SCIENCE APPLICATIONS INTL CORP ATTN: K SITES	ATTN: TIC
SCIENCE APPLICATIONS INTL CORP ATTN: TECH LIBRARY	TRW S I G
SCIENCE APPLICATIONS INTL CORP ATTN: G BINNINGER	ATTN: N GUILS
SRI INTERNATIONAL ATTN: DR JIM GRAN	TRW SPACE & DEFENSE SECTOR
ATTN: E UTHE	ATTN: W WAMPLER
ATTN: J GIOVANOLA	W J SCHAFFER ASSOCIATES, INC
ATTN: J SIMONS	ATTN: D YOUMANS
ATTN: M SANAI	ATTN: W BUITENHUYS
TECH REPS, INC ATTN: F MCMULLAN	WASHINGTON STATE UNIVERSITY ATTN: PROF Y GUPTA
TECHNICO SOUTHWEST INC ATTN: S LEVIN	WEIDLINGER ASSOC, INC ATTN: H LEVINE
TITAN CORPORATION ATTN: J ROCCO	WEIDLINGER ASSOCIATES, INC ATTN: T DEEVY
ATTN: J THOMSEN	WEIDLINGER ASSOCIATES, INC ATTN: I SANDLER
	ATTN: M BARON
	WILLIAMSON AIRCRAFT CO ATTN: WILLIAMSON